Check for updates

Received: 16 February 2024 | Revised: 7 June 2024 | Accepted: 13 July 2024

DOI: 10.1002/suco.202400219

ARTICLE

fib CEB-FIP WILEY

Shear and interface shear fatigue of semi-precast slabs with lattice girders under cyclic loading

Matthias Hillebrand | **Annkathrin Sinning** | **Josef Hegger**

Institute of Structural Concrete, RWTH Aachen University, Aachen, Germany

Correspondence
Matthias Hillebrand, Institute of Structural Concrete, RWTH Aachen University, Mies-van-der-Rohe-Strasse 1, 52074 Aachen, Germany.
Email: mhillebrand@imb.rwth-aachen.de

Funding information
German Federation of Industrial Research Association, Grant/Award Number: 20580N; Federal Ministry for Economic Affairs and Climate Action

Abstract

More and more often, semi-precast reinforced concrete slabs with lattice girders are employed for industrial buildings or bridges, where they are exposed to high cycle fatigue loading. Despite research in recent years that has led to the formulation of an *S–N* curve for lattice girders, the effects of cyclic loading on semi-precast slabs have not yet been sufficiently clarified. Moreover, research has so far been limited to single-span slabs. The effects of continuous slab systems, which are mainly realized in buildings and bridges, cannot be considered in the calculation of fatigue resistance yet. To improve the fatigue design concept for shear and interface shear, theoretical and experimental investigations were conducted at the Institute of Structural Concrete, RWTH Aachen University. In addition to the fatigue behavior of 16 tests under cyclic loading, particular attention is paid to the increase in shear and interface shear resistance at the inner support of continuous slabs. Furthermore, the influences of the support detailing were investigated. The findings illustrate further potential for optimization of the design under cyclic loading.

KEYWORDS

cyclic loading, fatigue, interface shear, lattice girder, semi-precast slab, shear

1 | INTRODUCTION

Due to their high cost-efficiency and flexibility, around 70% of all floor slabs in German buildings and industrial constructions are made of semi-precast reinforced concrete slabs with lattice girders.[1] The lower parts of these slabs are prefabricated in the factory and completed with *in situ* concrete at the construction site. On the one hand, semi-precast elements reduce the need for costly formwork, and on the other hand, the cast-in-place concrete in combination with the lattice girders creates a monolithic structural behavior of the slab.

In precast construction, the lattice girders serve both as transport and assembly support in the construction stage and as interface shear and/or shear reinforcement in the ultimate limit state. While slabs in buildings are mainly loaded by quasi static loads, in industrial structures, for example, due to fork-lift trucks, and in bridges, cyclic fatigue loads have to be considered. The effects of cyclic loading, especially on the interface between the precast and *in situ* concrete and on the fatigue strength of the lattice girders, have not been sufficiently clarified. In previous tests, it was shown that the expected stress ranges in the lattice girder were experimentally not achieved.[2] From these fatigue tests, *S–N* curves for lattice girder types have recently been developed.[2,3] However, fundamental investigations are still missing in order to explain the smaller stress range observed in tests and to improve the design concept since the current design approaches for shear and

This is an open access article under the terms of the Creative Commons Attribution License, which permits use, distribution and reproduction in any medium, provided the original work is properly cited.
© 2024 The Author(s). *Structural Concrete* published by John Wiley & Sons Ltd on behalf of International Federation for Structural Concrete.

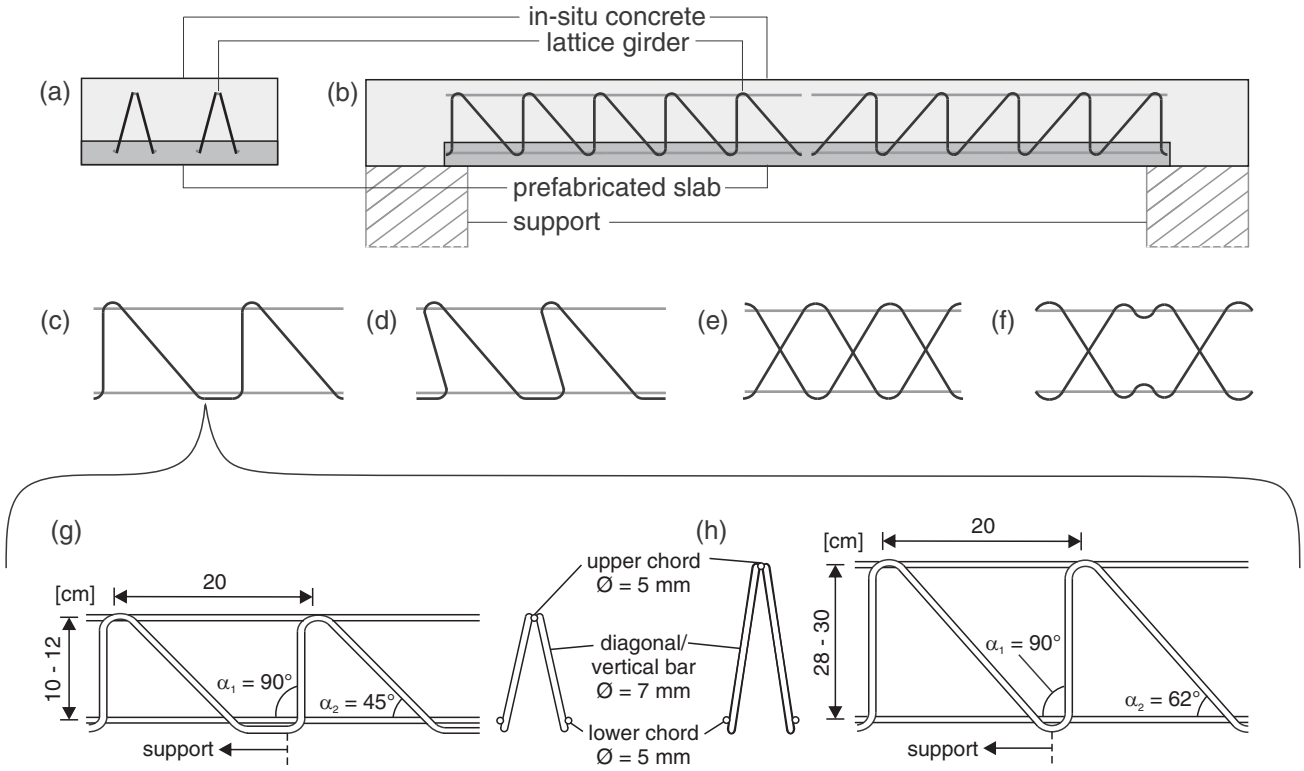


FIGURE 1 (a) cross section and (b) longitudinal section of a semi-precast slab; longitudinal section of lattice girders approved for fatigue in semi-precast slabs (c–e) and semi-precast walls (c, f); details of the lattice girders investigated here in thin slabs (g) and thick slabs (h).

interface shear fatigue lead to high required shear reinforcement ratios and thus uneconomical results.

While semi-precast slabs are placed as single-span slabs in the construction phase, the layer of *in situ* concrete connects them to a statically indeterminate continuous slab system. The favorable influence of a continuous slab system on the shear and interface shear resistance of semi-precast slabs with lattice girders, as has already been determined for monolithic slabs without and with low shear reinforcement ratios,[4–6] has not yet been investigated and is consequently not considered in the current design approaches.

To improve the design concept for shear and interface shear in semi-precast slabs with lattice girders, theoretical and experimental investigations were conducted at the Institute of Structural Concrete (in German: Institut für Massivbau, IMB), RWTH Aachen University. The investigations under monotonic loading have already been presented in Hillebrand and Hegger.[7] This paper presents the tests under cyclic fatigue loading.

2 | THEORETICAL BACKGROUND

2.1 | Lattice girders

In semi-precast construction, lattice girders act as interface reinforcement between a precast element and *in situ* concrete (Figure 1a,b). Depending on their design, they can also be used as shear or punching shear reinforcement. The actual load-bearing capacities of lattice girders are not adequately covered by Eurocode 2 (EC2) and were therefore additionally regulated in Germany by a Technical Approval (TA; in German: Allgemeine bauaufsichtliche Zulassung, AbZ). This enables higher load-bearing capacities to be applied in combination with EC2 while complying with all necessary safety standards. The approval is comparable to the European Technical Approval. Whereas many types of lattice girders exist for monotonic loading, only four types of lattice girders are approved for fatigue loading in Germany (Figure 1c–f). These types are described in TA and offered by a small number of manufacturers.[8–15] A comprehensive overview of lattice girders and their use in semi-precast slabs is given in Furche and Bauermeister.[1]

The lattice girder in Figure 1c, known as EQ[9] or KTS,[11] is designed to resist high monotonic and cyclic shear and interface shear forces in semi-precast slabs and semi-precast walls.

For this reason, it is used in many semi-precast slabs and therefore it was selected for the investigations presented here. Furthermore, an *S–N* curve is available (Figure 2), which allows an optimized design and a more

17517648, 0, Downloaded from https://onlinelibrary.wiley.com/doi/10.1002/suco.202400219 by Rwth Aachen Hochschulbibliothek, Wiley Online Library on [19/08/2024]. See the Terms and Conditions (https://onlinelibrary.wiley.com/terms-and-conditions) on Wiley Online Library for rules of use; OA articles are governed by the applicable Creative Commons License

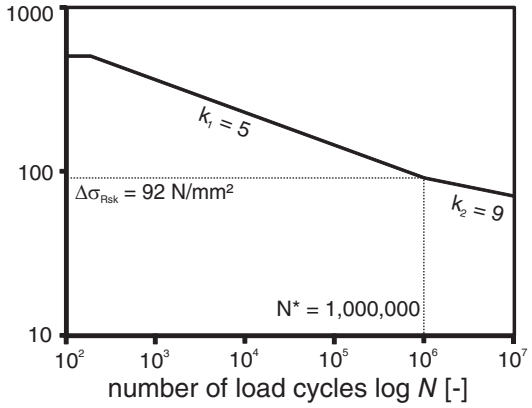


FIGURE 2 *S–N* curve for lattice girders EQ/KTS according to Technical Approvals.[9,11]

accurate evaluation of the presented tests. Details of the selected lattice girders are given in Figure 1g,h. An overview of further research on lattice girders and in particular their use under high cycle fatigue loading is summarized in Hillebrand et al.[2]

2.2 | Interface shear

The interface shear design of semi-precast slabs with lattice girders under cyclic loading in Germany is regulated by TA, which are based on EC2 combined with the National Annex of Germany (EC2 + NA(D)).[16,17] For fatigue design, the acting shear force range of the slab has to comply with the shear resistance (Equation 1), which is based on the stress ranges in the diagonal and vertical bars of the lattice girders according to the *S–N* curve shown in Figure 2 and the expected number of load cycles.

The interface shear fatigue resistance of the lattice girders according to TA is verified using Equation (2), whose derivation is based on the design for monotonic loading. Additional details for the design are given in Hillebrand et al.[2] The design formulas according to EC2 (Equation 3),[16] EC2 + NA(D) (Equation 4),[17] and the draft of the new Eurocode 2 (prEC2) (Equation 5)[18] serve for comparison. These design concepts and their backgrounds are discussed explicitly in Wieneke.[19]

$$\frac{\Delta V_{Ed}}{z \times b_i} \leq \Delta v_{Rdi,} \tag{1}$$

$$\text{TA}: \Delta v_{Rdi} = \sum_{i \geq 1} \rho_{w,i} \times \frac{\Delta\sigma_{Rsk}}{\gamma_{s,fat}} \times (1.4 \times \sin\alpha_i + 1.67 \times \cos\alpha_i), \tag{2}$$

$$\text{EC2}: \Delta v_{Rdi} = 0.5 \times c \times f_{ctd} + \sum_{i \geq 1} \rho_{w,i} \times \frac{\Delta\sigma_{Rsk}}{\gamma_{s,fat}} \times (\mu \times \sin\alpha_i + \cos\alpha_i), \tag{3}$$

$$\text{EC2} + \text{NA(D)}: \Delta v_{Rdi} = \sum_{i \geq 1} \rho_{w,i} \times \frac{\Delta\sigma_{Rsk}}{\gamma_{s,fat}} \times (1.2 \times \mu \times \sin\alpha_i + \cos\alpha_i), \tag{4}$$

$$\text{prEC2}: \Delta v_{Rdi} = \sum_{i \geq 1} \rho_{w,i} \times \frac{\Delta\sigma_{Rsk}}{0.45 \times \gamma_{s,fat}} \times (\mu \times \sin\alpha_i + \cos\alpha_i), \tag{5}$$

with: ΔV_{Ed}, shear force range; Δv_{Rdi}, range of the shear fatigue resistance of the interface; $\rho_{w,i}$ interface reinforcement ratio $\rho_{w,i} = A_{si}/A_i$; A_{si}, area of steel reinforcement crossing the interface including shear reinforcement from shear design with sufficient anchorage at both sides of the interface; A_i, area of the interface; $\Delta\sigma_{Rsk}$; characteristic resistance to fatigue according to *S–N* curve; $\gamma_{s,fat}$, partial safety factor of reinforcement under fatigue $\gamma_{s,fat} = 1.15$; α_i, inclinations of bars of reinforcement in accordance with Figure 1g,h; f_{ctd}, design value of the tensile strength of concrete; c, coefficient of adhesion; μ, coefficient of friction.

2.3 | Shear

For the verification of the shear reinforcement under cyclic fatigue loading, a truss model is used in analogy to the design under monotonic loading. Under cyclic loading, a reduction of the concrete contribution by aggregate interlock is assumed due to the local degradation of the concrete along the shear cracks.[20] As a result, steeper compression strut inclinations are assumed (Equation 6), resulting in a lower calculated fatigue resistance (Equation 7). Recent investigations indicate that this approach is too conservative.[21–23] Currently, this approach is used in EC2, EC2 + NA(D), prEC2, and TA, with different determinations of the compression strut inclination θ. For non-prestressed members, $\cot\theta$ can be chosen freely within the limits of Equation (8) according to EC2 and prEC2, while in EC2 + NA(D) and TA, the adjusted limits according to Equation (9) apply.

$$\cot\theta_{fat} = \sqrt{\cot\theta,} \tag{6}$$

$$\Delta V_{Ed} \leq \frac{\Delta\sigma_{Rsk}}{\gamma_{s,fat}} \times a_{sw} \times z \times \sum_{i \geq 1} (\cot\theta_{fat} + \cot\alpha_i) \times \sin\alpha_i, \tag{7}$$

17517648, 0, Downloaded from https://onlinelibrary.wiley.com/doi/10.1002/suco.202400219 by Rwth Aachen Hochschulbibliothek, Wiley Online Library on [19/08/2024]. See the Terms and Conditions (https://onlinelibrary.wiley.com/terms-and-conditions) on Wiley Online Library for rules of use; OA articles are governed by the applicable Creative Commons License

$$1.0 \leq \cot\theta \leq 2.5, \tag{8}$$

$$1.0 \leq \cot\theta \leq \frac{1.2}{1 - V_{\mathrm{Rd,cc}}/V_{\mathrm{Ed}}} \leq 3.0, \tag{9}$$

$$V_{\mathrm{Rd,cc}} = 0.24 \times f_{\mathrm{ck}}^{1/3} \times b \times z, \tag{10}$$

with: θ, inclination of the concrete compression strut to the slab axis under monotonic loading; θ_{fat}, inclination of the concrete compression strut to the slab axis under cyclic fatigue loading; a_{sw}, cross-sectional area of the provided shear reinforcement; z, inner lever arm; $V_{\mathrm{Rd,cc}}$, concrete contribution; V_{Ed}, design value of the applied shear force.

2.4 | Shear slenderness

The design equations for shear and interface shear resistance of semi-precast slabs with lattice girders were derived and verified by single-span slab tests with concentrated loads and transferred to continuous systems without any adjustments. However, a significant influence of shear slenderness on the shear resistance of beams and slabs was observed in refs.[5,24–30]

The shear capacity of a member increases with decreasing shear slenderness. It is generally described by Equation (11). For single-span elements with two concentrated loads, Equation (11) leads to the simplification in Equation (12), where the shear slenderness is the ratio of the distance a between the load introduction and the support and the effective depth d.

$$\lambda = \frac{M}{V \times d}, \tag{11}$$

$$\lambda = \frac{a}{d}. \tag{12}$$

For the same a/d ratio, the shear slenderness at internal supports of continuous elements is significantly smaller than that for single-span members or end supports of slabs.[7] This also implies a larger shear resistance at inner supports due to the transfer by direct compression struts to the support.

3 | EXPERIMENTAL INVESTIGATIONS

3.1 | Test program

To address remaining open questions from the previous investigations[2,31–33] as well as new issues, for example, the influence of shear slenderness on shear capacity, experimental investigations were conducted. Thirty-two test specimens manufactured at the Institute of Structural Concrete (IMB) were tested as an extension of an investigation on the shear and interface shear behavior of semi-precast slabs with lattice girders. Sixteen test specimens were subjected to monotonic loading[7] and served as reference tests for another 16 identical slabs that were tested under high cycle fatigue loading. Table 1 gives an overview of the test program. The tests were divided into the Series 3 and 4 with respect to the slab depth. Series 1 and 2 have already been tested in a previous research project.[2,31] Series 1 was the predecessor of Series 3, with the same slab depth. Series 2 was the predecessor of Series 4, also with the same slab depth. Series 1 and 2 differ from 3 and 4 in particular in the design at the supports, as explained in Section 3.2. For Series 1 and 2, only tests on single-span slabs with cyclic loading were carried out. In Series 3 and 4, in addition to further tests on single-span slabs under cyclic loading, supplementary reference tests were carried out with monotonic loading and/or on single-span slabs with cantilevers, whose results have already been published in Hillebrand and Hegger.[7]

3.2 | Test specimens

The test specimens of Series 3 had a total depth of 16 cm, including the 6 cm thick precast slab, which corresponds to the minimum depth for cyclic loading according to the TA. The test specimens of Series 4 had a depth of 34 cm, with a precast slab of 7 cm. The width of all slabs was 85 cm. All test specimens were produced at the IMB. The planned roughness of the prefabricated slabs was achieved through a brush stroke after concreting. To investigate the pure resistance of the interface shear reinforcement, for the test specimens EG19a, EG19b, EG20c, and EG20d, the adhesion and friction of the interface were eliminated almost completely by smoothing the fresh concrete and curing the surface with grease.

The roughness was measured using the sand patch method according to Kaufmann[34] and laser measurements with the ELAtextur measuring device from IWS Messtechnik. The laser measurements were additionally conducted because the sand patch method, which is the most popular method, sometimes produces user-dependent results.[35] Figure 3a provides an overview of all measured surface roughnesses. An example of the roughened surface is shown in Figure 3b. Figure 3c gives an overview of the concrete cylinder strength measured for the prefabricated slabs and the *in situ* concrete.

The lattice girders were used as shear and interface shear reinforcement. Two shear or interface shear

17517648, 0, Downloaded from https://onlinelibrary.wiley.com/doi/10.1002/suco.202400219 by Rwth Aachen Hochschulbibliothek, Wiley Online Library on [19/08/2024]. See the Terms and Conditions (https://onlinelibrary.wiley.com/terms-and-conditions) on Wiley Online Library for rules of use; OA articles are governed by the applicable Creative Commons License

TABLE 1 Test program.

Tests		Support condition		Shear reinforcement ratio		Concrete strength		Surface roughness (mm)	Overall depth (cm)		Diameter Ø longitudinal reinforcement (mm)	
		s.span	Cont.	Low	High	C25	C50		16	34	15	20
Series 3	EG15a	X		X		X		alm. rough	X		X	
	EG15b		X	X		X		alm. rough	X		X	
	EG16c	X		X		X		alm. rough	X		X	
	EG16d		X	X		X		alm. rough	X		X	
	EG17a	X			X	X		alm. rough	X		X	
	EG17b		X		X	X		alm. rough	X		X	
	EG18c	X			X	X		alm. rough	X		X	
	EG18d		X		X	X		alm. rough	X		X	
	EG19a	X		X		X		v. smooth	X		X	
	EG19b		X	X		X		v. smooth	X		X	
	EG20c	X		X		X		v. smooth	X		X	
	EG20d		X	X		X		v. smooth	X		X	
	EG21a	X			X		X	alm. rough	X		X	
	EG21b		X		X		X	alm. rough	X		X	
	EG22c	X			X		X	alm. rough	X		X	
	EG22d		X		X		X	alm. rough	X		X	
Series 4	EG23a	X		X		X		alm. rough		X		X
	EG23b		X	X		X		alm. rough		X		X
	EG24c	X		X		X		alm. rough		X		X
	EG24d		X	X		X		alm. rough		X		X
	EG25a	X			X	X		alm. rough		X		X
	EG25b		X		X	X		alm. rough		X		X
	EG26c	X			X	X		alm. rough		X		X
	EG26d		X		X	X		alm. rough		X		X
	EG27a	X			X		X	alm. rough		X		X
	EG27b		X		X		X	alm. rough		X		X
	EG28c	X			X		X	alm. rough		X		X
	EG28d		X		X		X	alm. rough		X		X
	EG29a	X		X		X		alm. rough		X		X[a]
	EG29b		X	X		X		alm. rough		X		X
	EG30c	X		X		X		alm. rough		X		X[a]
	EG30d		X	X		X		alm. rough		X		X

Abbreviations: alm. rough, almost rough ($R_t \leq 1.5$ mm); cont., continuous slab ($\lambda = 2.5$); EG, Ermüdung Gitterträger (German; English Translation: Fatigue Lattice Girder); a, single-span slab with monotonic loading; b, continuous slab with monotonic loading; c, single-span slab with cyclic loading; d, continuous slab with cyclic loading; high, high shear reinforcement ratio (four rows); low, low shear reinforcement ratio (two rows); s.span: single-span slab ($\lambda = 4.0$); v. smooth, very smooth.

[a]Single-span slab with top longitudinal reinforcement.

reinforcement ratios were tested. Figure 4a shows the low reinforcement ratio with two rows of lattice girders ($\rho_w = 1.8‰$), where the upper transverse and longitudinal reinforcement may be stacked on the lattice girders according to TA.[9,11] In slabs with a high shear reinforcement ratio (Figure 4b), four rows of lattice girders, $\rho_w = 3.6‰$, the upper longitudinal reinforcement has to be placed at the level of the upper chord of the lattice

17517648, 0, Downloaded from https://onlinelibrary.wiley.com/doi/10.1002/suco.202400219 by Rwth Aachen Hochschulbibliothek, Wiley Online Library on [19/08/2024]. See the Terms and Conditions (https://onlinelibrary.wiley.com/terms-and-conditions) on Wiley Online Library for rules of use; OA articles are governed by the applicable Creative Commons License

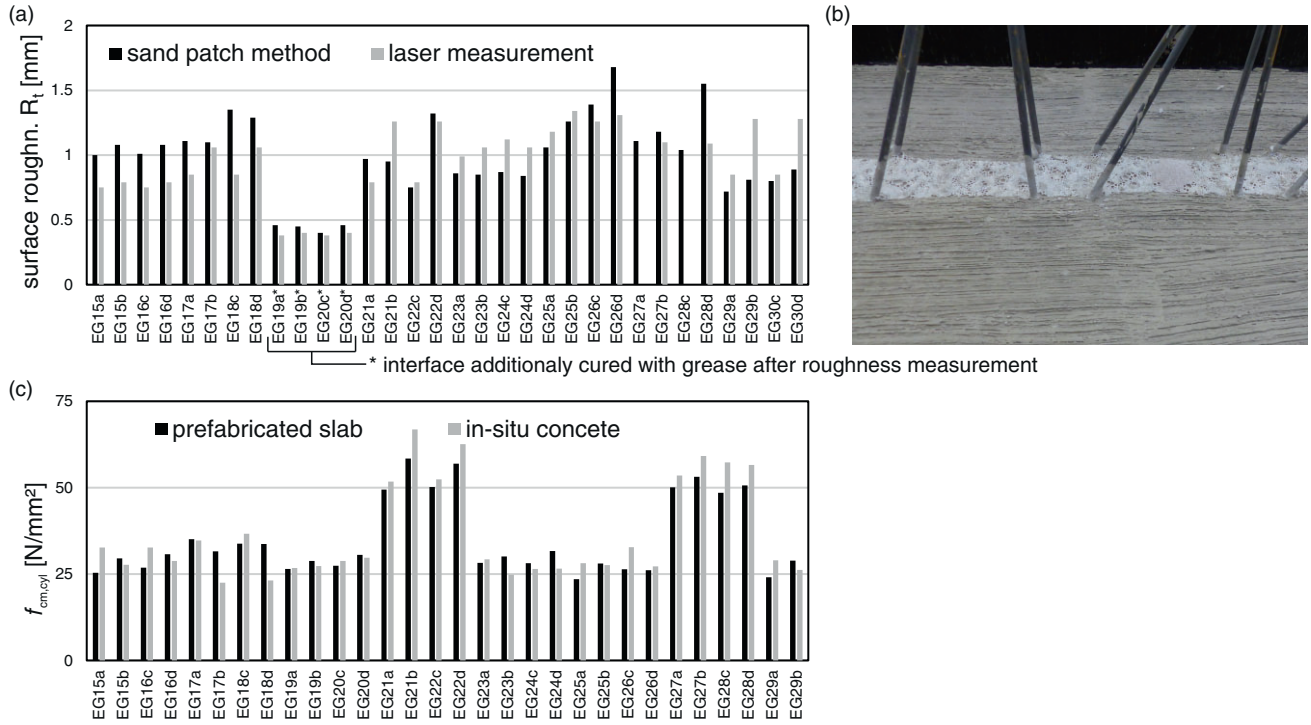


FIGURE 3 Overview of (a) measured roughness R_t and (b) surface roughness of slab EG24c and (c) concrete strength of prefabricated slabs and *in situ* concrete.

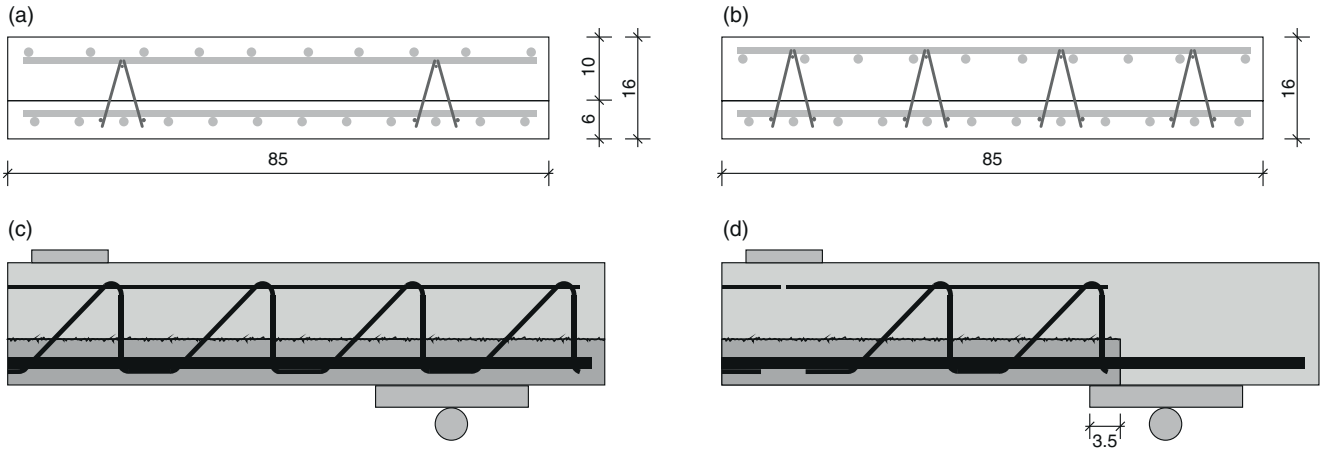


FIGURE 4 Arrangement of the upper longitudinal and transverse reinforcement with (a) low and (b) high shear reinforcement ratio; (c) detailing of support in refs.[2,32]; (d) detailing of support in current investigation.

girders, while the transverse reinforcement may still be placed above the lattice girder.

A smooth reinforcing steel (type B500) was used for the lattice girders. The upper and lower chords of the lattice girders consisted of a bar with diameter Ø = 5 mm, the vertical and diagonal bars were made of a diameter Ø = 7 mm (Figure 1g,h). The average yield strength of diagonal and vertical bars was $f_y = 520\ \mathrm{N/mm^2}$. More information on the yield and tensile strength of the lattice girders used is given in Hillebrand and Hegger.[7] To avoid flexural failure, high-strength bars (type S900/1100, $f_y = 900\ \mathrm{N/mm^2}$) with diameter Ø = 15 mm and Ø = 20 mm were used as longitudinal reinforcement. Table 2 gives an overview of the dimensions and geometrical parameters of the test specimens.

In the previous project,[2,32] the interface between the precast slab and the *in situ* concrete was provided along the entire slab length (Figure 4c). In the tests presented here, according to the usual construction on site, the precast slab was placed only 3.5 cm onto the support. The

17517648, 0, Downloaded from https://onlinelibrary.wiley.com/doi/10.1002/suco.202400219 by Rwth Aachen Hochschulbibliothek, Wiley Online Library on [19/08/2024]. See the Terms and Conditions (https://onlinelibrary.wiley.com/terms-and-conditions) on Wiley Online Library for rules of use; OA articles are governed by the applicable Creative Commons License

TABLE 2 Dimensions and geometrical parameters of the test specimens in Series 3 and 4.

	Series 3		Series 4	
	Single-span	**Continuous**	**Single-span**	**Continuous**
Dimensions ($l/b/h$) (cm)	170/85/16	240/85/16	384/85/34	542/85/34
Thickness prefabricated slab/*in situ* concrete (cm)	6/10	6/10	7/27	7/27
Effective depth d (cm)	13.3	13.3	31.0	31.0
Distance support to load a (cm)	50	50	130	130
Shear slenderness λ (−)	4	2,5	4	2,5
Lattice girder (−)	EQ/KTS	EQ/KTS	EQ/KTS	EQ/KTS
Low shear reinforcement ratio ρ_l (‰)	1.8	1.8	1.8	1.8
High shear reinforcement ratio ρ_l (‰)	3.6	3.6	3.6	3.6
Diameter Ø longitudinal reinforcement (mm)	15	15	20	20
Longitudinal reinforcement ratio ρ_l (%)	2.0	2.0	2.0	2.0

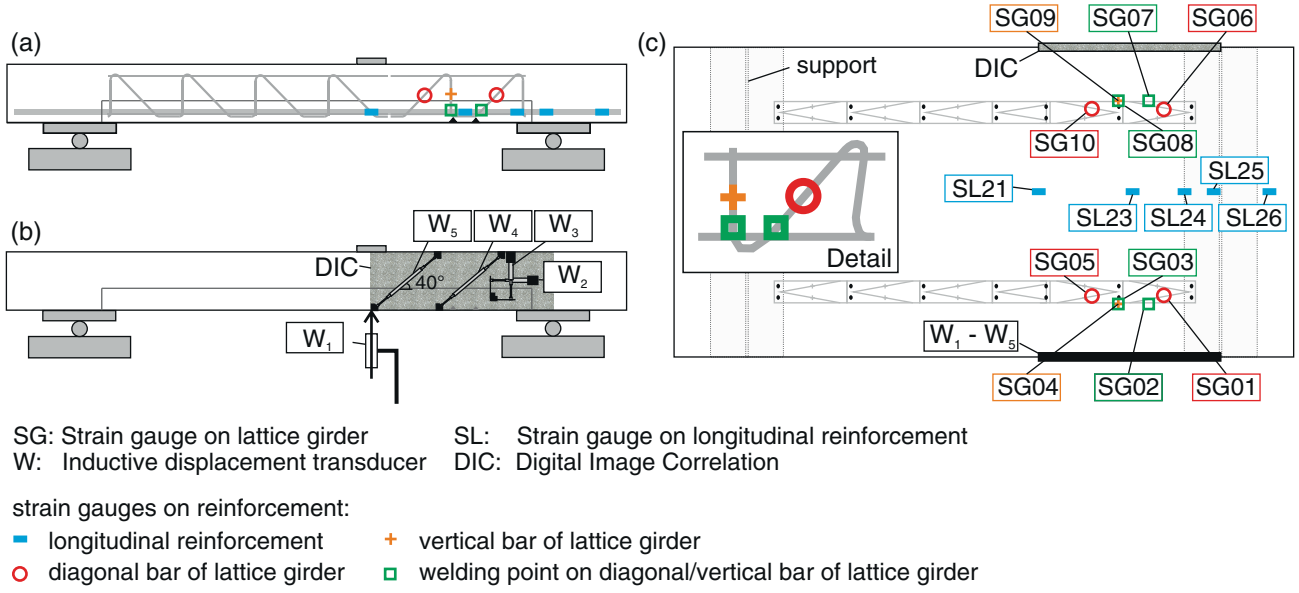


FIGURE 5 Overview of the installed measurement instrumentation for EG20c: (a, b) section/side view; (c) top view with detail of strain gages on lattice girders.

longitudinal reinforcement protruded from the prefabricated slab into the *in situ* concrete. In this area, the *in situ* concrete is poured over the entire slab depth (Figure 4d).

The continuous recording of the behavior of the slabs during the test was carried out using strain gages, inductive displacement transducers, and a Digital Image Correlation (DIC) system. The strain gages were attached to the lattice girders on the vertical and diagonal bars. As the bars have reduced fatigue strength due to welding in the area of the weld, measurements were taken in the center of each bar and near the bottom weld point. An additional strain gage was applied to the longitudinal reinforcement below the load introduction (SL21). In some tests, a few more measurements were made on this longitudinal reinforcement near the support to observe the anchorage of the longitudinal reinforcement. The opening and displacement of the interface were also measured with one displacement transducer each. The DIC was used to measure displacements along cracks or the interface. Figure 5 shows the arrangement of the measurement instrumentation as an example for a Series 3 slab.

Since the slabs with cyclic loading were constructed and tested identically to the reference slabs, further information about the test specimens (including reinforcement, concrete, the production, and the measurement instrumentation) is given in Hillebrand and Hegger.[7] Details of all slabs can be found in the test report.[36]

17517648, 0, Downloaded from https://onlinelibrary.wiley.com/doi/10.1002/suco.202400219 by Rwth Aachen Hochschulbibliothek, Wiley Online Library on [19/08/2024]. See the Terms and Conditions (https://onlinelibrary.wiley.com/terms-and-conditions) on Wiley Online Library for rules of use; OA articles are governed by the applicable Creative Commons License

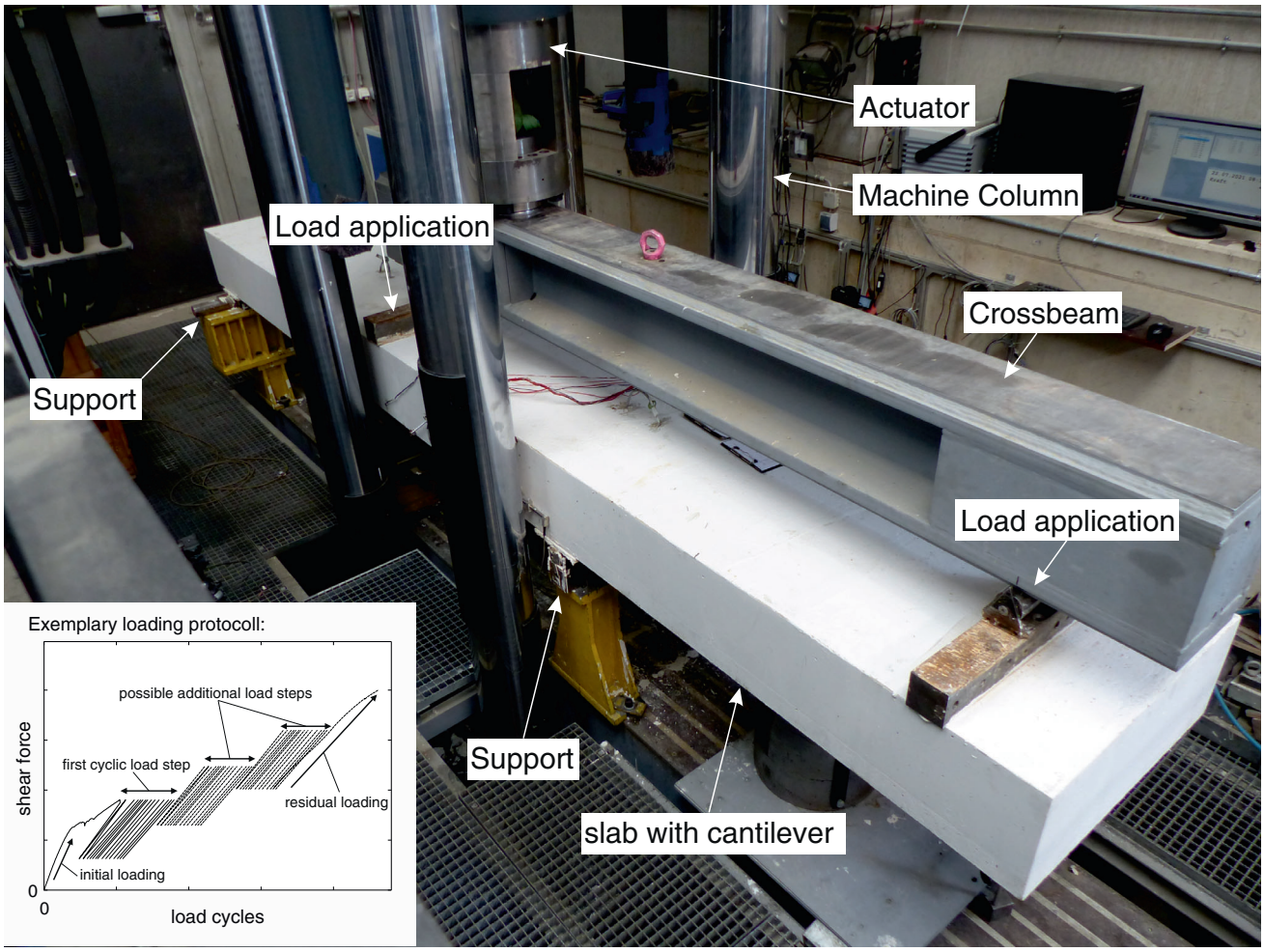


FIGURE 6 Real test setup using the example of a slab with cantilever.

3.3 | Test setup

The cyclic tests were carried out using a servo-hydraulic testing machine HB5000 from Zwick/Roell (Figure 6). To avoid constraints, the test specimens were supported by two steel rollers. For Series 3 slabs with a depth of 16 cm, the load was applied at a distance of 0.5 m from the support; the load distance for Series 4 slabs with a depth of 34 cm was 1.3 m (Figure 7). The loads were applied over the entire width of the slabs.

To investigate the influence of shear slenderness on shear resistance, single-span and continuous slabs with constant load distances a were investigated. This resulted in a shear slenderness of $\lambda = 4.0$ for the single-span slabs and $\lambda = 2.5$ (according to Equation 11) for continuous slabs. The continuous slabs, designed as slabs with protruding cantilever, were loaded with a load F_k at the cantilever that was increased linearly with the test load at the inner span F to achieve continuous action while keeping the shear slenderness constant throughout the test. Furthermore, effects resulting from static indeterminacy in a real, continuous system are avoided. The resulting internal forces are shown in Figure 8.

A cyclic test was always preceded by a monotonic test. The monotonic tests served as a reference in terms of structural behavior and to estimate the level of the cyclic loading. The monotonic tests were presented in detail in Hillebrand and Hegger.[7]

The upper cyclic load was defined between 50% and 85% of the monotonic resistance from the reference test. The lower cyclic load was determined in order to obtain calculated stress ranges according to the design equation of TA[9,11] in the diagonal bars of the lattice girders of approximately $\Delta\sigma = 200$ N/mm^2. If a slab failure did not occur during the cyclic loading, the levels of the maximum and minimum loading were increased, keeping the stress range in the diagonal bars of the lattice girders constant (Figure 6). If no failure of the slabs was achieved after load increase the load range was increased. If fatigue failure was still not achieved, the tests were stopped after about five to 6 million load cycles and the residual monotonic shear resistance was determined.

17517648, 0, Downloaded from https://onlinelibrary.wiley.com/doi/10.1002/suco.202400219 by Rwth Aachen Hochschulbibliothek, Wiley Online Library on [19/08/2024]. See the Terms and Conditions (https://onlinelibrary.wiley.com/terms-and-conditions) on Wiley Online Library for rules of use; OA articles are governed by the applicable Creative Commons License

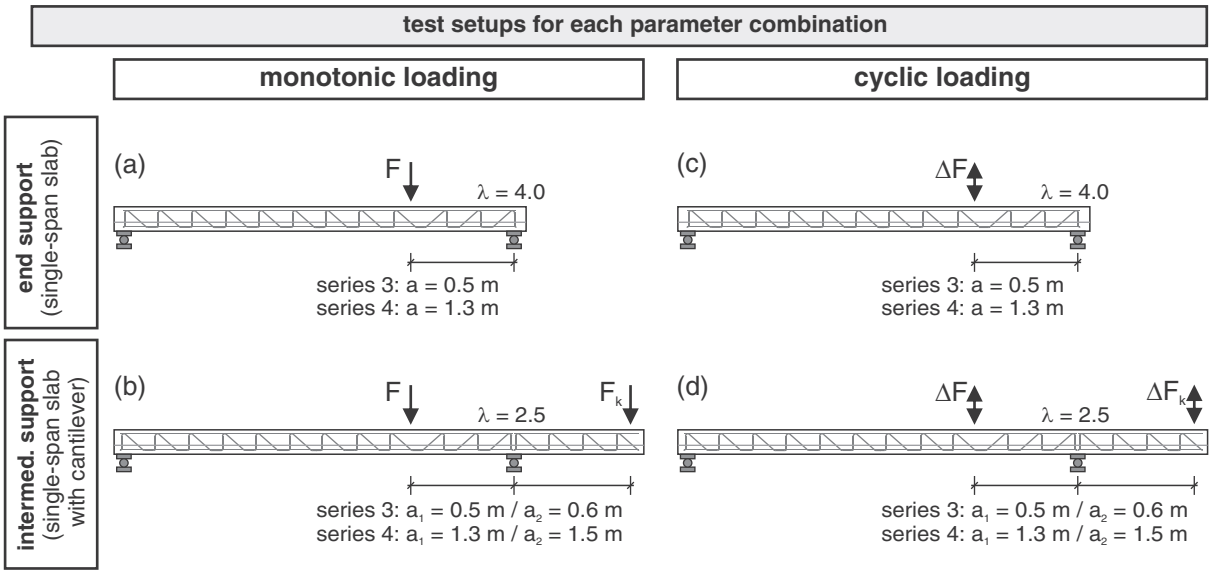


FIGURE 7 Schematic test setups of the monotonic and cyclic tests.

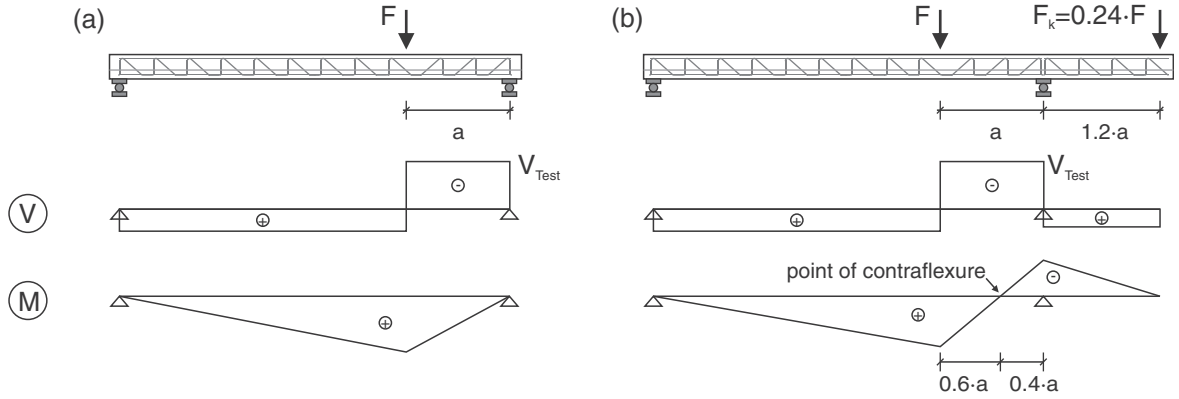


FIGURE 8 Load and internal forces on (a) single-span slabs and (b) slabs with cantilever.

The cyclic loading of the tests was carried out in a force-controlled manner, while a monotonic loading was carried out in a displacement-controlled manner.

3.4 | Test results

3.4.1 | Overview of results

Table 3 provides an overview of the loads of the cyclic tests based on the reference tests.[7] It contains the data of the first and last load step as well as the number of load cycles reached, the reason of failure and, if a fatigue failure was not obtained, the residual monotonic resistance. A detailed list for each test, including intermediate load stages can be found in Hegger and Hillebrand.[36]

According to Table 3, a calculated stress range $\Delta\sigma_{calc}$ of the shear reinforcement of at least 200 N/mm^2 was generally targeted at the beginning of the test. Employing the *S*–*N* curve according to TA (Figure 2), the stress range of 200 N/mm^2 corresponds to calculated 21,000 load cycles. The upper cyclic loads of the tests corresponded to approximately 55%–86% of the monotonic resistance of the reference tests.

For the thin test specimens of Series 3 ($h = 16$ cm, EG16–EG22), the residual monotonic resistances were determined after several million load cycles, since no indication of a failure due to cyclic loading was visible. For some of the thick test specimens of Series 4 ($h = 34$ cm, EG24–EG30), an anchorage failure occurred after some hundreds of load cycles, causing a premature end of the test.

3.4.2 | Structural behavior

The structural behavior under cyclic loading is explained using the example of test specimen EG22c. It was selected

17517648, 0, Downloaded from https://onlinelibrary.wiley.com/doi/10.1002/suco.202400219 by Rwth Aachen Hochschulbibliothek, Wiley Online Library on [19/08/2024]. See the Terms and Conditions (https://onlinelibrary.wiley.com/terms-and-conditions) on Wiley Online Library for rules of use; OA articles are governed by the applicable Creative Commons License

TABLE 3 Overview of loads and endured load cycles of the cyclic tests.

	V_{ref} (kN)	$V_{max,1}/V_{ref}$ (−)	$\Delta\sigma_{calc,1}$ (N/mm²)	N_1 (−)	$V_{max,f}/V_{ref}$ (kN)	$\Delta\sigma_{calc,f}$ (N/mm²)	N_f (−)	N_{tot} (−)	Failure (−)	V_{Res}/V_{ref} (−)
EG16c	253	0.75	220	2.5×10^6	-	-	-	$2.5 \cdot 10^6$	$S+$	1.02
EG16d	321	0.73	230	1.2×10^6	0.73	460	0.1×10^6	1.3×10^6	S_A	-
EG18c	288	0.52	215	1.1×10^6	0.78	215	2.6×10^6	6.1×10^6	$S+$	1.19
EG18d	293	0.72	231	2.6×10^6	0.80	231	2.9×10^6	5.5×10^6	$S+$	1.01
EG20c	208	0.60	219	1.1×10^6	0.72	329	2.8×10^6	4.9×10^6	(I,F)+	1.11
EG20d	197	0.66	229	3.0×10^6	0.66	328	1.8×10^6	6.6×10^6	(I,F)+	1.12
EG22c	353	0.64	235	1.5×10^6	0.78	235	3.7×10^6	6.0×10^6	$S+$	1.07
EG22d	434	0.75	234	1.6×10^6	0.86	292	1.7×10^6	5.3×10^6	$S+$	1.07
EG24c	363	0.55	188	1.7×10^6	0.67	188	4.7×10^6	6.4×10^6	S_A+	1.03
EG24d	386	0.65	219	2.7×10^6	0.81	264	1.0×10^6	6.3×10^6	S_A+	1.10
EG26c	434	0.73	229	15,700	-	-	-	15,700	S_A	-
EG26d	533	0.75	250	300	-	-	-	300	S_A	-
EG28c	538	0.70	223	4.8×10^6	-	-	-	4.8×10^6	S_A+	-
EG28d	686	0.73	243	0.3×10^6	-	-	-	0.3×10^6	S_A	-
EG30c	383	0.78	265	1190	-	-	-	1190	S_A	-
EG30d	420	0.74	262	0.9×10^6	-	-	-	0.9×10^6	S_A	-

Note: V_{ref}: shear resistance of reference test; $V_{max,1}$: maximum load in first load level; $\Delta\sigma_{calc,1}$: calculated stress range of the lattice girders according to EC2 + NA(D)/TA; N_1: number of load cycles of the first load level; $V_{max,f}$: Maximum load at failure/test stop; $\Delta\sigma_{calc,f}$: calculated stress range of the lattice girders according to EC2 + NA(D)/TA; N_f: number of load cycles at the last load level; N_{tot}: total number of load cycles (sum of $N_1 + ... + N_f$; intermediate load levels are given in Hegger and Hillebrand[36]); *I*: interface shear failure; *S*: shear failure due to failure of vertical and/or diagonal bars; S_A: shear failure due to anchorage failure of lattice girder; *F*: fatigue failure of diagonal/vertical bars; +: residual resistance tested; V_{Res}: residual resistance.
Abbreviations: EC2, Eurocode 2; TA, Technical Approval.

because test specimen EG22d showed similar behavior with changed shear slenderness and otherwise the same properties, making it suitable for analyzing the influence of shear slenderness in chapter 3.4.3. Other test specimens will also be considered later on to describe other influencing parameters.

The slab EG22c was initially loaded up to a shear force of 225 kN. This corresponded to 64% of the resistance of the identical monotonic reference test, EG21a. At this point, only small bending cracks had formed at the bottom of the slab. The deflection under the load introduction was 4.8 mm (Figure 9b), and the measured strain of the longitudinal reinforcement at this position was 2.2‰. The strains of the lattice girders were small and far below the yield strength.

After the initial monotonic loading, the cyclic loading (Figure 10) started with an upper load of $V_{max} = 225$ kN and a lower load of $V_{min} = 125$ kN, resulting in a calculated stress range in the lattice girders of $\Delta\sigma_{calc} = 235$ N/mm² according to TA. After approximately 1.5 million load cycles, the load level was increased to $V_{max} = 250$ kN and to $V_{min} = 150$ kN because of minimal cracking and low measured stress ranges (e.g., measurement point SG02: $\Delta\sigma_{test,SG02} = 50$ N/mm²) (Figure 10d). After another approximately 2.3 million load cycles, the load level was increased again. The new upper load of $V_{max} = 275$ kN corresponds to 78% of the resistance from the monotonic reference test, and the minimum load was $V_{min} = 175$ kN. At this load level, deflection, crack width, and steel stresses increased abruptly, accompanied by the formation of a shear crack (Figure 10a). The stress range in the lattice girder increased only slightly (e.g., SG02: approximately 60 N/mm²) and remained below the calculated stress range. The bearable number of load cycles using this measured stress range in the lattice girder, calculated with the *S*–*N* curve of TA, is approximately 46 million load cycles. The cyclic loading was stopped after a total of 6.06 million load cycles.

Since there were no indications of fatigue failure after 6.06 million load cycles, the residual monotonic resistance was tested. For this purpose, the test was unloaded and reloaded to failure. It could be observed that despite the unloading to 0 kN, both a part of the deflection and the crack width remained (Figure 11). This was also observed for the measured steel strains (e.g., SG02: remaining strain approximately 1‰). Finally, the test specimen EG22c was monotonically loaded to failure. At about 300 kN, the crack width increased

17517648, 0, Downloaded from https://onlinelibrary.wiley.com/doi/10.1002/suco.202400219 by Rwth Aachen Hochschulbibliothek, Wiley Online Library on [19/08/2024]. See the Terms and Conditions (https://onlinelibrary.wiley.com/terms-and-conditions) on Wiley Online Library for rules of use; OA articles are governed by the applicable Creative Commons License

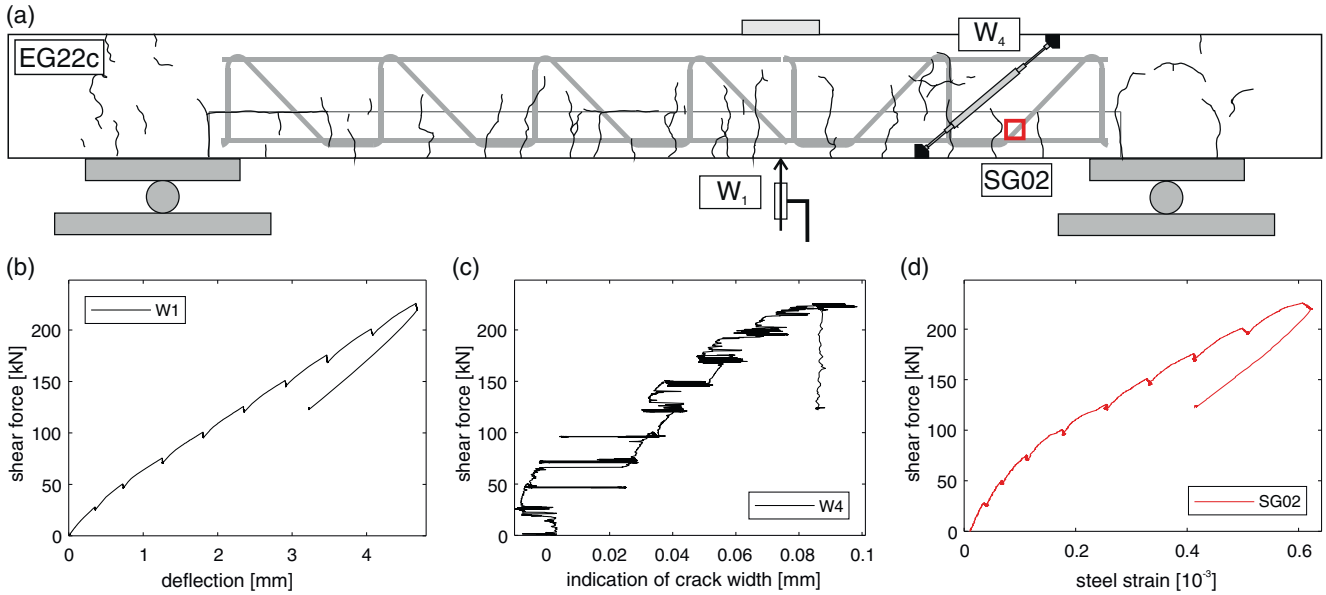


FIGURE 9 Test EG22c: (a) Crack pattern after initial monotonic loading, (b) deflection, (c) indication of crack width, and steel strain at initial monotonic loading.

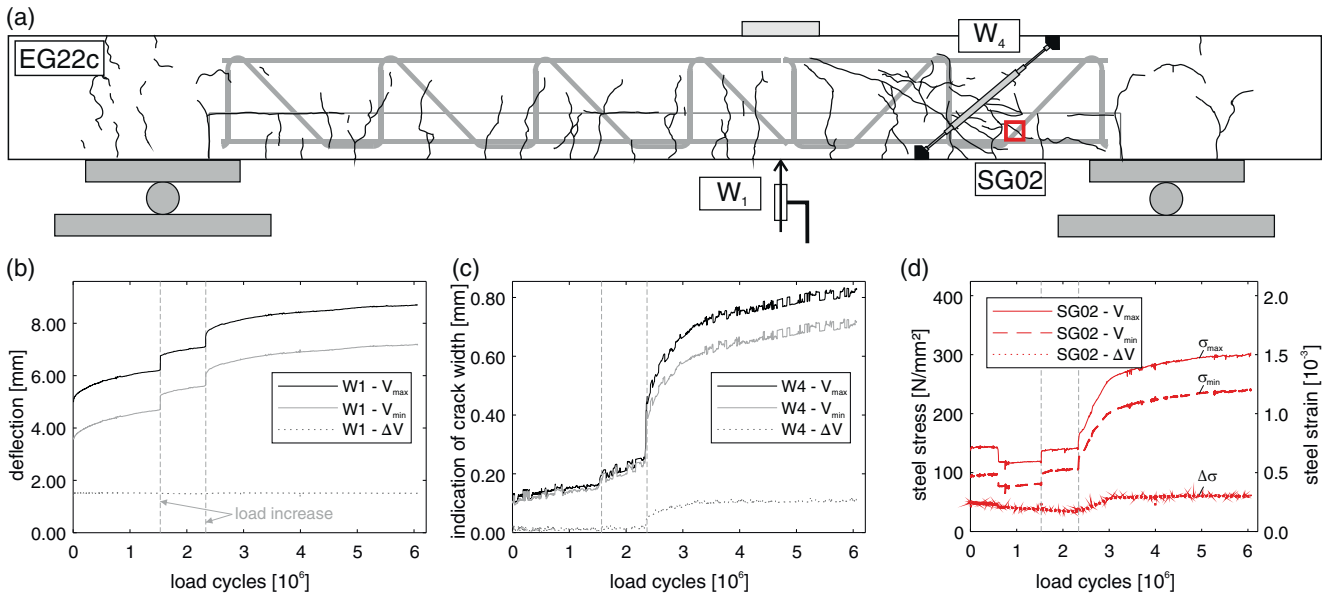


FIGURE 10 Test EG22c: (a) Crack pattern after cyclic fatigue loading, (b) deflection, (c) indication of crack width, and (d) steel strain at cyclic loading.

overproportionately and measurement point SG02 indicated yielding of the diagonal bar of the lattice girder. The failure load of 379 kN was about 7% higher than in the monotonic reference test.

After the cyclic loading, the evaluation of the crack patterns of all test specimens already showed a high similarity with the monotonic reference tests. Figure 12 compares the crack development between the identical slabs EG17a (reference test with monotonic loading) and EG18c (test with cyclic loading).

The residual shear resistance was tested in the case of nine out of 16 cyclic tests. Table 3 demonstrates that the preceding cyclic loading had no negative effect on the residual shear resistance of the test specimens in these tests. In individual tests, the resistance was even up to 19% higher than in the monotonic test.

17517648, 0, Downloaded from https://onlinelibrary.wiley.com/doi/10.1002/suco.202400219 by Rwth Aachen Hochschulbibliothek, Wiley Online Library on [19/08/2024]. See the Terms and Conditions (https://onlinelibrary.wiley.com/terms-and-conditions) on Wiley Online Library for rules of use; OA articles are governed by the applicable Creative Commons License

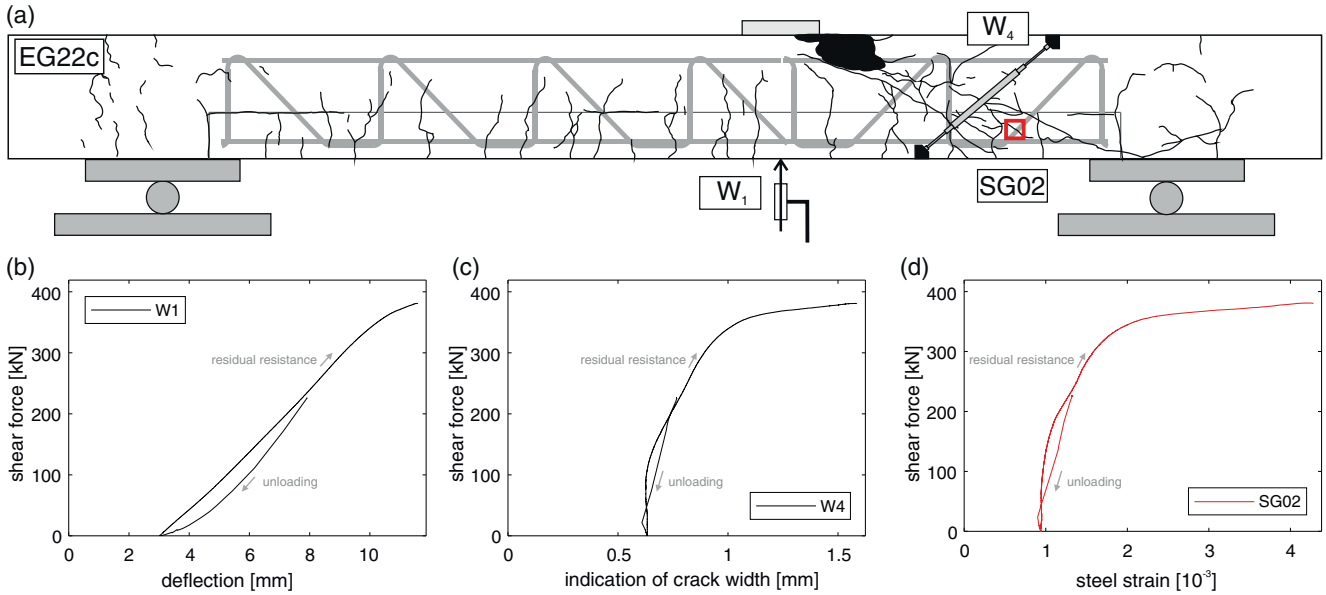


FIGURE 11 Test EG22c: (a) Crack pattern after testing residual shear resistance, (b) deflection, (c) indication of crack width, and (d) steel strain at testing of residual shear resistance.

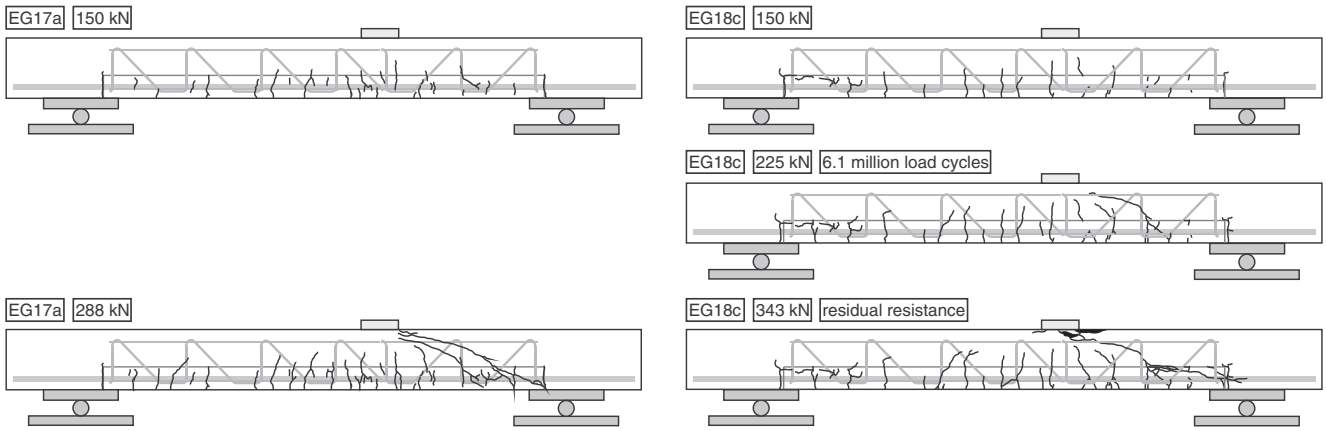


FIGURE 12 Crack patterns of the test with monotonic loading EG17a (left) and the test with cyclic loading EG18c (right).

Figure 13 compares the shear crack development of the monotonically loaded test specimen EG21b with the shear crack development of the cyclic test specimen EG22d during the initial monotonic loading, the cyclic loading, and the determination of the residual shear resistance. At initial loading (up to 325 kN), the indicated crack widths of both test specimens are very similar. During the period of cyclic loading with an increased upper load of 375 kN, the crack width increased significantly. After several million load cycles, the slab EG22d was completely unloaded, with a remaining crack width of 0.4 mm (W_5) to 0.6 mm (W_4). During the subsequent reloading, only a slight increase in crack width was measured even beyond the previous maximum load of 375 kN. At about 450 kN a strong increase in the shear crack width was observed, and the crack development followed the curve of the monotonic reference test. Similar behavior was found in refs.[37–39] for concrete cylinders subjected to cyclic compressive loading. This underlines the finding that the preceding cyclic loading did not affect the monotonic shear resistance of the test specimen.

3.4.3 | Influence of shear slenderness

For the tests under cyclic loading, different crack patterns of the slabs with cantilever (EG22d) were observed compared to the single-span slabs (EG22c; Figure 14). In the span of test specimen EG22c, the initial flexural and flexural shear cracks from the initial monotonic loading developed further under cyclic loading until a dominant

17517648, 0, Downloaded from https://onlinelibrary.wiley.com/doi/10.1002/suco.202400219 by Rwth Aachen Hochschulbibliothek, Wiley Online Library on [19/08/2024]. See the Terms and Conditions (https://onlinelibrary.wiley.com/terms-and-conditions) on Wiley Online Library for rules of use; OA articles are governed by the applicable Creative Commons License

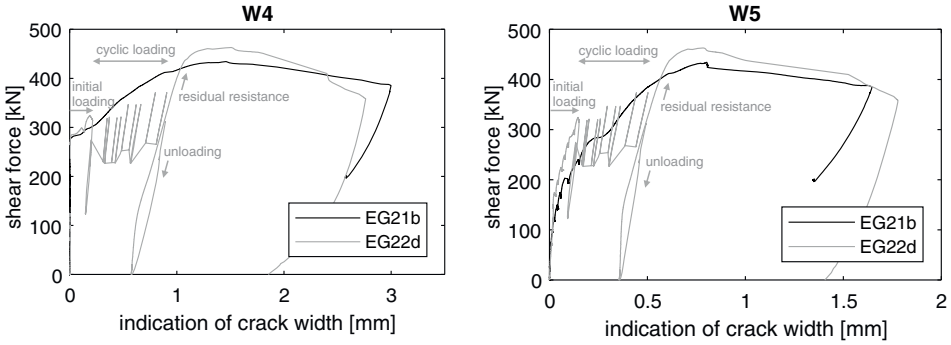


FIGURE 13 Comparison of the indicated shear crack width of the monotonic tests (EG21b) with the indicated shear crack width during initial loading, cyclic loading and the determination of the residual shear resistance of the cyclic tests (EG22d).

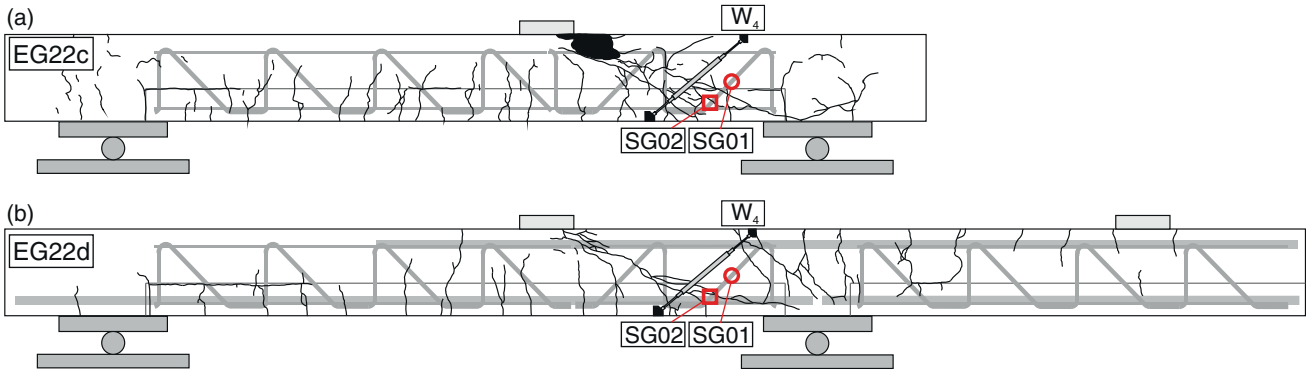


FIGURE 14 Crack patterns of tests (a) EG22c and (b) EG22d after determination of the residual shear resistance.

shear crack had formed. In the slabs with a cantilever, flexural cracks developed not only at the bottom side below the load introduction, but also at the top of the slab above the intermediate support due to the hogging moment. In the slabs with cantilever, an almost uncracked zone remained between the intermediate support and the load introduction, where a part of the shear force could be transferred via a direct concrete compression strut. The same behavior was found for the monotonic tests.[7]

The thin slabs of Series 3, with the exception of EG16c and EG16d, reached 5 million load cycles or more. Test EG16c had to be stopped early due to a machine failure and was finished by testing the residual shear resistance. Test EG16d failed prematurely during cyclic loading, as presumably the anchorage of the lattice girders failed due to the very high applied stress range ($\Delta\sigma_{calc} = 460$ N/mm^2). A failure of the other test specimens of Series 3 did not occur after several increases of the load level as well as the stress range.

The cyclic loading of the slabs with cantilever was at a similar or larger load level in the last load step compared to the loads of the corresponding single-span slabs (Table 3). However, the strains of the lattice girders were lower for the test specimens with cantilever than for the single-span slabs. As in the monotonic tests,[7] this observation can be explained by the changed load transfer due to the smaller shear slenderness, as shown, for example, by the strain measurements SG01 and SG02 of the lattice girder in Figure 15. While the upper load of EG22c (single-span slab) in the last load step was $V_{max} = 275$ kN, EG22d (continuous slab) had already reached $V_{max} = 375$ kN. In spite of the higher upper load, the measured steel stresses of the continuous slab EG22d were smaller.

The test specimen EG22d achieved a 23% higher residual shear resistance compared to the single-span slab EG22c, which is in agreement with the results of the reference tests of EG21a and EG21b (Table 3,[7]). The tests EG24c and EG24d from Series 4 confirm this behavior. A reduction of the monotonic shear resistance due to preceding cyclic loading could not be deducted from the test results.

3.4.4 | Influence of the shear reinforcement ratio

According to the investigations in the previous project,[2,31,33] the degree of shear and interface shear reinforcement have a significant influence on the crack pattern and the type of failure. In test specimens with two

17517648, 0, Downloaded from https://onlinelibrary.wiley.com/doi/10.1002/suco.202400219 by Rwth Aachen Hochschulbibliothek, Wiley Online Library on [19/08/2024]. See the Terms and Conditions (https://onlinelibrary.wiley.com/terms-and-conditions) on Wiley Online Library for rules of use; OA articles are governed by the applicable Creative Commons License

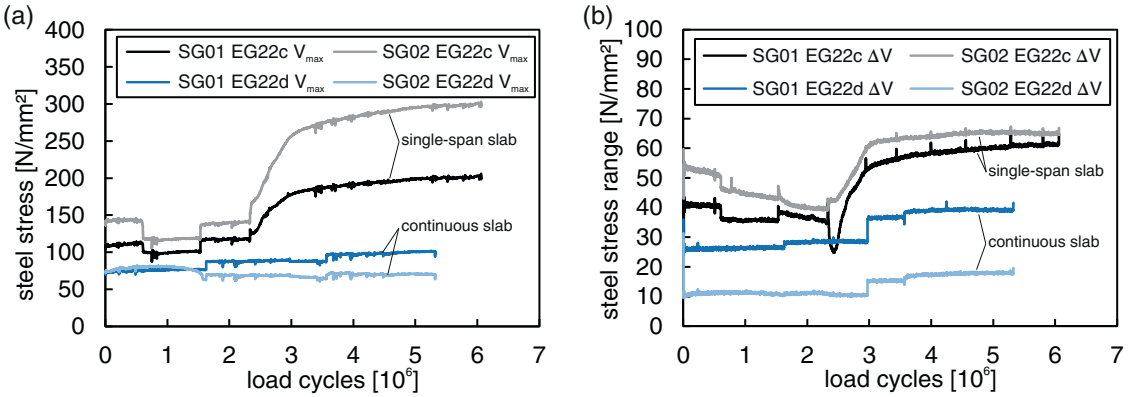


FIGURE 15 Comparison of EG22c and EG22d: (a) steel stresses at upper load and (b) stress ranges ($\Delta\sigma = \sigma_{max} - \sigma_{min}$).

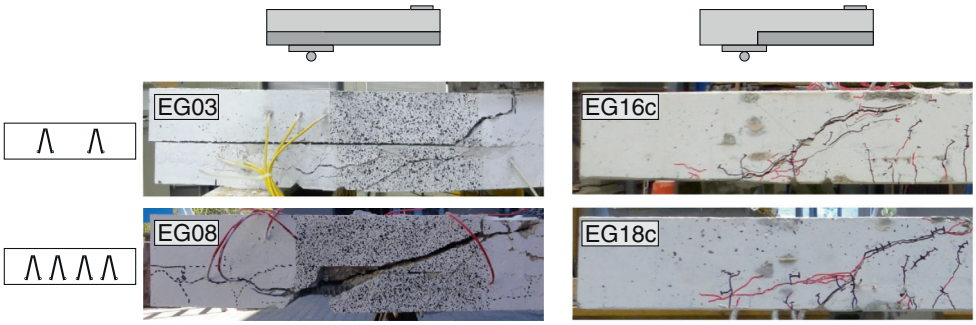


FIGURE 16 Comparison of crack patterns according to reinforcement ratio and support detail (EG03 and EG08 from Hegger and Wieneke[32]).

rows of lattice girders the interface failed (Figure 16, upper left side), while shear failure occurred at higher reinforcement ratios (Figure 16, lower left side). It should be noted that these test specimens were designed with a continuous interface, according to Figure 4c. In the current tests with the support design according to Figure 4d, shear failure was observed in both cases (Figure 16, right side). A dependence of the reinforcement ratio could not be determined anymore. Further investigations into the support detail will be presented in Section 3.4.7.

3.4.5 | Influence of concrete compressive strength

During the cyclic tests, no influence of the concrete compressive strength on the shear resistance of the test specimens could be detected. The test specimens EG18c (C25) and EG22c (C50) were, apart from the concrete strength, identical in construction. Both were able to withstand several million load cycles without showing any indication of failure. The load level of the last load step and the resulting stress ranges in the reinforcement were in similar ranges. Similar results were observed for the slabs with cantilever EG18d and EG22d. Moreover, no differences in crack patterns were observed. For both concrete strengths, no cracking occurred at the interface. Accordingly, no influence of the concrete strength on the adhesion could be detected.

3.4.6 | Influence of the overall slab depth

In the monotonic tests, anchorage failure of the vertical and diagonal lattice girders occurred in the area of the failure causing shear crack, in particular, with the thick slabs of Series 4 ($h = 34$ cm).[7] The approach of a reduced usable yield strength $f_y = 420$ N/mm^2, which is regulated in the TA taking into account the poorer bond of the smooth diagonals, was confirmed by these tests. The cyclic tests also confirm this finding. In most cases, the thick slabs ($h = 34$ cm) failed after significantly fewer load cycles than the thin slabs ($h = 16$ cm). This effect had already been observed in the previous project.[2,32,40] Since the relative load level was set similarly for thick and thin slabs, the resulting measured stress ranges in the lattice girders of Series 4 were not particularly larger. As no fatigue failures of the lattice girders could be detected, it is assumed that the cyclic tests on thick slabs predominantly failed by an anchorage failure.

17517648, 0, Downloaded from https://onlinelibrary.wiley.com/doi/10.1002/suco.202400219 by Rwth Aachen Hochschulbibliothek, Wiley Online Library on [19/08/2024]. See the Terms and Conditions (https://onlinelibrary.wiley.com/terms-and-conditions) on Wiley Online Library for rules of use; OA articles are governed by the applicable Creative Commons License

3.4.7 | Influence of interface roughness and support detailing

For slabs under cyclic loading, a rough surface of the precast slab of at least $R_T = 1.5$ mm is required, according to TA. Although the applied roughness depth R_T was generally less than 1.5 mm (Figure 3) in the cyclic tests, no crack displacements parallel to the interface were observed. In contrast to Series 1 and 2 from the previous project,[2] the interface was not extended along the entire length of the slab (Figure 4c). In the current tests, the prefabricated slab rested on the support only for a few centimeters (Figure 4d). To investigate the influence of the interface roughness and the influence of the support detailing under cyclic loading, the slabs EG20c and EG20d were therefore produced with a very smooth interface (R_T <0.4 mm).

After the initial loading of slab EG20c, the interface was cracked along the entire interface (Figure 17b). During the cyclic loading, a horizontal displacement of the interface of about 1.2 mm was measured. As in the monotonic tests with a smooth interface,[7] vertical cracks on the top side of the slab developed as an extension of the vertical interface between the *in situ* concrete and the prefabricated slab (Figure 17b, green mark). In test EG16c with a rough interface and identical detailing, no such cracking occurred (Figure 17a). The cause of cracking on the top side above the support under cyclic loading is shown in Figure 18. As a result of the cracking of the interface, the cyclic loading leads to the displacement of the top concrete. As this displacement is interfered by the longitudinal reinforcement anchored in the *in situ* concrete, tensile stresses occur on the top side of the slab, leading to the crack formation in Figure 17b. A comparison with the crack pattern of slab EG03 from Hegger and Wieneke[32] (Figure 17c) underlines this effect. Since the interface along the entire length was cracked in this test, an additional contribution of the longitudinal reinforcement by an arching effect was not possible. As a result of the cyclic loading, the failure of the lattice girders led to free sliding of the *in situ* concrete, which resulted in the failure of the slab.

Such sliding was prevented in slab EG20c by the modified support detailing, although the lattice girders had

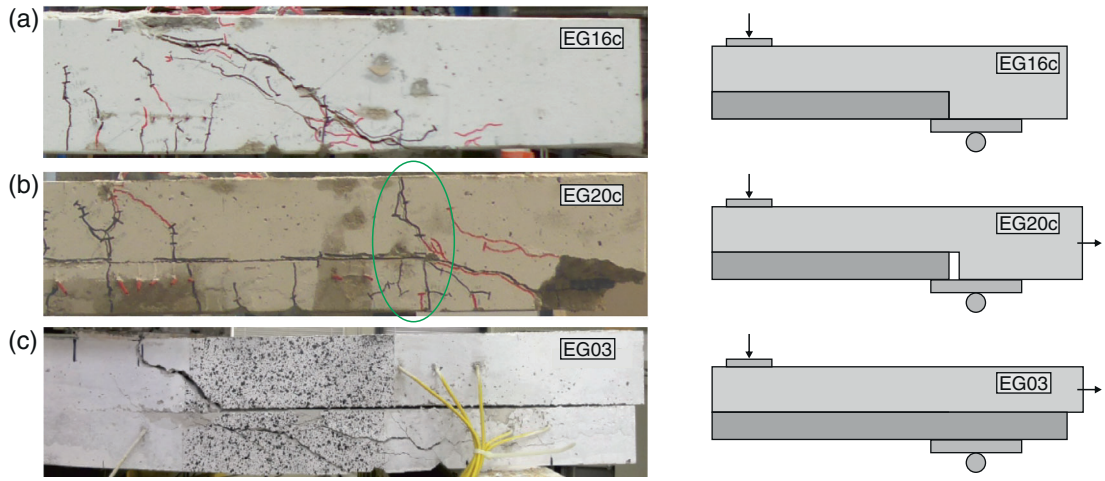


FIGURE 17 Crack pattern and displacement figure: (a) EG16c (almost rough interface, $R_T = 1.0$ mm) after test of residual shear resistance, (b) EG20c (very smooth interface, R_T <0.4 mm) after test of residual shear resistance, and (c) EG03 (smooth interface, $R_T = 0.6$ mm) after cyclic failure (from Hegger and Wieneke[32]).

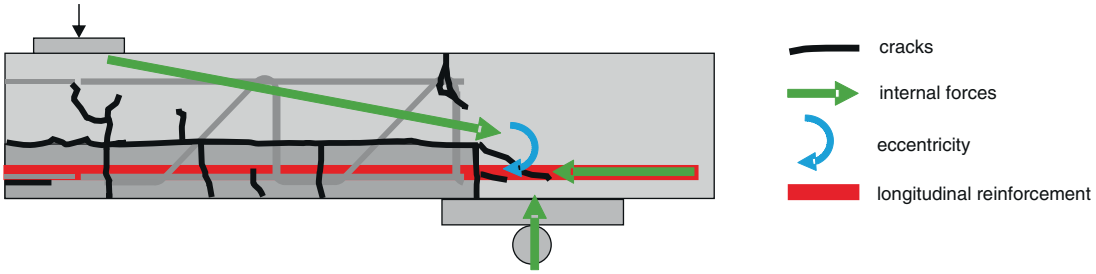


FIGURE 18 EG20c: shear transfer by arching effect due to *in situ* concrete at the end of cyclic loading.

17517648, 0, Downloaded from https://onlinelibrary.wiley.com/doi/10.1002/suco.202400219 by Rwth Aachen Hochschulbibliothek, Wiley Online Library on [19/08/2024]. See the Terms and Conditions (https://onlinelibrary.wiley.com/terms-and-conditions) on Wiley Online Library for rules of use; OA articles are governed by the applicable Creative Commons License

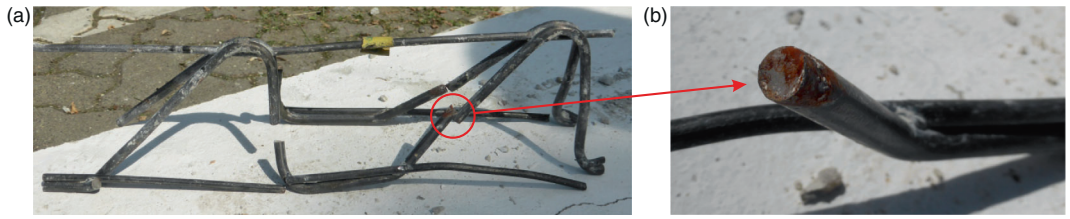


FIGURE 19 Test EG20c: (a) fatigue fractures of lattice girder; (b) fracture pattern of diagonal bar.

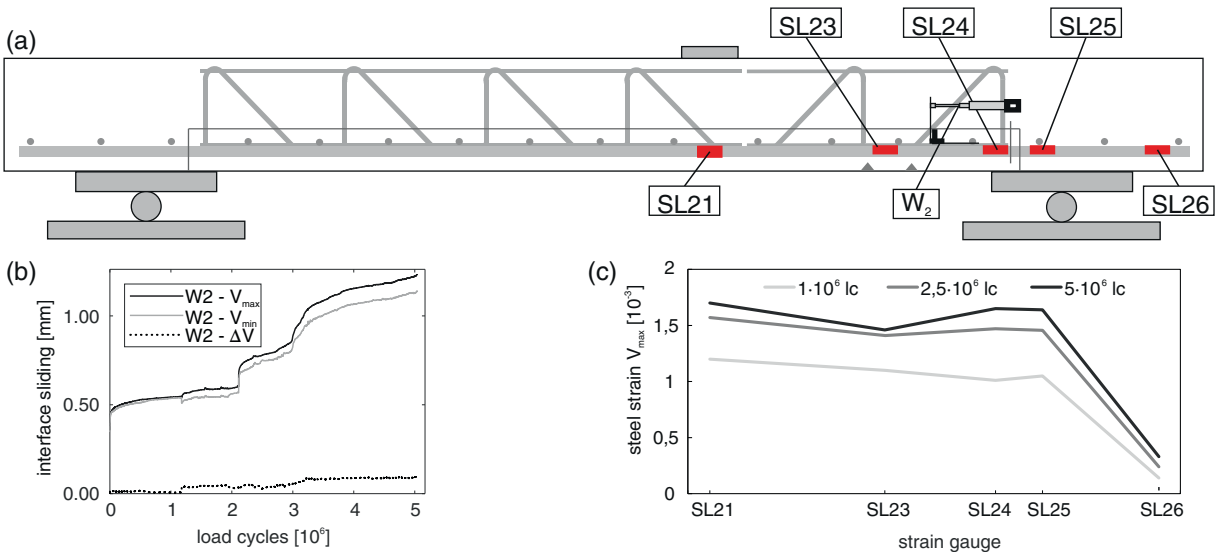


FIGURE 20 EG20c: (a) measuring instrumentation, (b) interface displacement, and (c) strains of longitudinal reinforcement.

fatigue fractures in their diagonal and vertical bars at the level of the interface after about 3 million load cycles (Figure 19), which in turn favored sliding. Despite the fatigue fractures of the lattice girders, slab EG20c was still able to endure the cyclic loading. Failure did not occur after 4.9 million load cycles until the residual shear resistance was tested. The residual shear resistance of EG20c was even higher than that of the structurally identical monotonic test EG19a. The modification of the support detail and the longitudinal reinforcement anchored in the concrete behind the support formed an additional load transfer mechanism through an arching effect, which explains the increase in shear resistance compared to the tests in Hegger and Wieneke.[32]

This unexpected but understandable effect can be confirmed by the strain measurement of the longitudinal reinforcement under cyclic loading at the upper load (Figure 20). The strain of the longitudinal reinforcement underneath the load introduction reached the highest values over the duration of the test (SL21). After 1 million load cycles, the measured strains of the longitudinal reinforcement did not decrease according to the course of the bending moment. They decline only at the support (SL23–26). Due to an enlargement of load, an increase in interface displacement was measured after 2 million load cycles. At about 3 million load cycles, another abrupt increase in interface displacement was observed, which was caused by fatigue failure of the lattice girders. At the same time, the strains of the longitudinal reinforcement increased in the immediate vicinity of the vertical interface at the support (SL24 and SL25) and were larger than in the shear span at SL23. This increase in strain of the longitudinal reinforcement at the support with a simultaneous increase in interface displacement illustrates the influence of the longitudinal reinforcement. While the interface sliding increased continuously throughout the test and the *in situ* concrete layer was pushed outwards, at the same time, shearing off of the two elements was prevented at the support by the longitudinal reinforcement anchored in the *in situ* concrete, and an arching effect was generated (Figure 18).

For the slab with cantilever EG20d, a complete crack along the interface was detected during the initial monotonic loading, too. The interface displacement increased during the cyclic loading, but was not as pronounced as for the single-span slab EG20c. No strain increase in the

17517648, 0, Downloaded from https://onlinelibrary.wiley.com/doi/10.1002/suco.202400219 by Rwth Aachen Hochschulbibliothek, Wiley Online Library on [19/08/2024]. See the Terms and Conditions (https://onlinelibrary.wiley.com/terms-and-conditions) on Wiley Online Library for rules of use; OA articles are governed by the applicable Creative Commons License

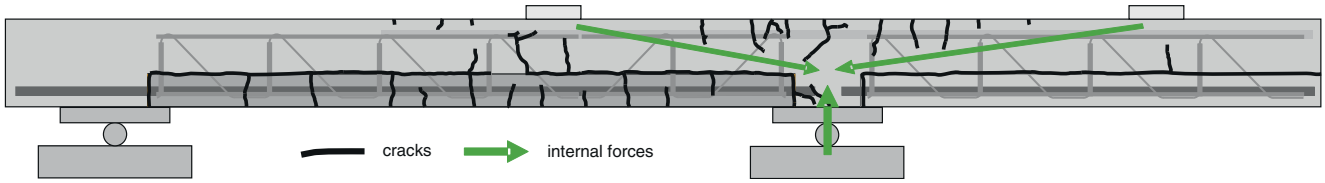


FIGURE 21 EG20d: Load transfer under cyclic loading with the cantilever slabs.

longitudinal reinforcement was observed at the vertical interface between the prefabricated slab and the *in situ* concrete. After more than 6 million load cycles and several fatigue failures of the lattice girder along the interface, a residual monotonic shear resistance in the range of the shear resistance of the monotonic reference test EG19b was determined. The favorable effect of deformation restraint by the longitudinal reinforcement observed for the slab EG20c was not necessary in EG20d. Instead, the arching effect was generated by the compression strut of the adjacent field (Figure 21).

3.4.8 | Steel stresses and steel failure

During the tests under cyclic loading, strain gages were used to record the stresses in the lattice girders (Figure 5). After the fatigue tests were completed, the test specimens were opened to check whether and at which locations the lattice girders had fatigue fractures. It was found that, with the exception of EG20c (Figure 19) and EG20d, no fatigue failure of the diagonal and vertical bars of the lattice girders occurred in the test specimens. In most of the test specimens, only fatigue failures of the lattice girders in the top and bottom chords in the immediate vicinity of the welds were observed. The reason for the missing fatigue failure of the diagonal and vertical bars of the lattice girders were the low stress ranges measured at the lattice girders.

The calculated stress ranges of at least 200 N/mm^2 could roughly be achieved in the tests with very smooth interfaces EG20c and EG20d only (Figure 22). Although the upper loads of many tests with rough interfaces were increased up to 80% of the monotonic resistance and the crack patterns were pronounced, the stress ranges determined from the strain gages were on average below 100 N/mm^2.

A redistribution process in the shear reinforcement, as also stated in Hillebrand and Hegger,[22] occurred, which is illustrated in Figure 22 for slab EG20c. At the beginning of the test, the maximum stress range was approximately $\Delta\sigma_{exp} = 100$ N/mm^2. After approximately 1.1 million load cycles, the shear range was increased by reducing the lower load, which led to a stress range of approximately $\Delta\sigma_{exp} = 150$ N/mm^2 (SG10). Although enlarging the load level after another 1 million load cycles with a constant shear range, an increase in the stress ranges was not observed. The following fatigue fractures of the lattice girder of EG20c were characterized by a failure of the diagonal and vertical bars at the level of the interface. First, the diagonal bar near measurement point SG10 failed at a measured stress range of approximately $\Delta\sigma_{exp} = 150$ N/mm^2 after 2.3 million load cycles. In the further course, after approximately 3 million load cycles, the stress ranges of SG06 and SG07 decreased abruptly to a stress range of approximately $\Delta\sigma_{exp} = 90$ N/mm^2 and $\Delta\sigma_{exp} = 130$ N/mm^2, respectively. As a result, the stress range at measurement point SG09 increased to $\Delta\sigma_{exp} = 75$ N/mm^2.

A reasonable cause for the low stress ranges in a large part of the test specimens are the remaining residual stresses and strains in the lattice girders at the lower loading, which were also observed during unloading prior to the test of the residual shear resistance (Figure 11). Sliding of the shear cracks during cyclic loading leads to degradation of the crack surface. As a result, this shear cracks can no longer close completely at the lower load due to wedging of the crack edges, and a residual strain remains in the lattice girders. To investigate this, partial unloading was performed on some cyclic tests at regular intervals. The test specimen EG16d was partially unloaded to a shear force of 30 kN after 1, 5000, 20,000, and 1,252,800 load cycles to measure the residual strains. Figure 23b shows the strain development after partial unloading at measurement point SG03. Already after the first load cycle, a high residual strain was measured. The strain at the upper load ($V_{max} = 235$ kN) was approximately 0.95‰ and at the lower load ($V_{min} = 182.5$ kN) about 0.9‰. After partial unloading to 30 kN, a residual strain of 0.44‰ remained. After 5000 load cycles, the strain had increased to 1.57‰ at the upper load and was 0.73‰ at unloading to 30 kN. The strains at the upper load and at a load of 30 kN had almost doubled compared to the first load cycle. The strain range between the maximum load and the partial unloading had increased from 0.51 to 0.84‰. However, these strain ranges are significantly smaller than the calculated values according to the design approaches.

17517648, 0, Downloaded from https://onlinelibrary.wiley.com/doi/10.1002/suco.202400219 by Rwth Aachen Hochschulbibliothek, Wiley Online Library on [19/08/2024]. See the Terms and Conditions (https://onlinelibrary.wiley.com/terms-and-conditions) on Wiley Online Library for rules of use; OA articles are governed by the applicable Creative Commons License

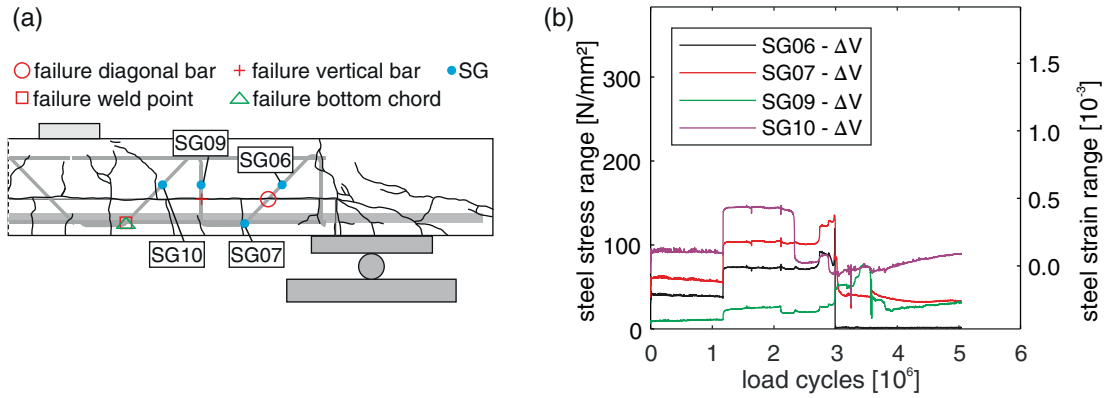


FIGURE 22 EG20c: (a) Crack pattern with lattice girder fractures and (b) steel stress ranges.

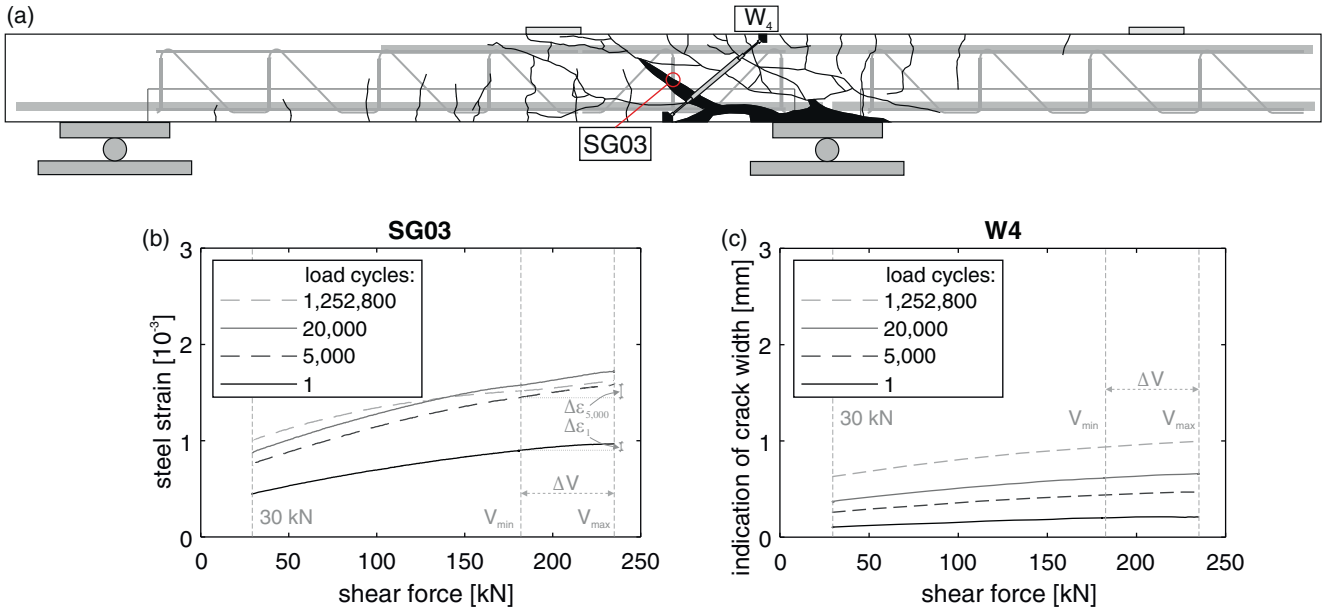


FIGURE 23 EG16d: (a) Measuring instrumentation, (b) steel strain at measurement point SG03, and (c) indication of crack width at measurement point W_4.

According to EC2 + NA(D) and TA, the strain range for $\Delta V = 205$ kN is $\Delta\varepsilon = 4.0‰$, which is clearly higher than the design yield strain. It can be assumed that residual strains would still remain in case of complete unloading, as the shear cracks cannot completely close due to the roughness of the crack surfaces. At 20,000 and 1,252,800 load cycles, there were still small increases in the strains.

This observation can be confirmed by evaluating the indication of the crack opening (measurement point W_4). As shown in Figure 23c, a slight decrease in the indicated crack widths was observed during partial unloading. A complete closure of the cracks at full unloading was not possible, as mentioned before. With an increasing number of load cycles, the remaining crack widths slightly increased.

The growth of steel strains with increasing load cycles, resulting from the degradation of the crack friction of the aggregate interlock of the shear cracks, is accounted for in the current standards by the use of a steeper compression strut angle (Equation 6). Residual strains in the shear reinforcement, which are caused by the incomplete closure of the shear cracks, have not been taken into account so far for the determination of stress ranges under cyclic loading.

4 | DATABASE

4.1 | Evaluation basics

To compare current design approaches, a database evaluation was carried out for the shear and interface shear design of semi-precast slabs with lattice girders under

17517648, 0, Downloaded from https://onlinelibrary.wiley.com/doi/10.1002/suco.202400219 by Rwth Aachen Hochschulbibliothek, Wiley Online Library on [19/08/2024]. See the Terms and Conditions (https://onlinelibrary.wiley.com/terms-and-conditions) on Wiley Online Library for rules of use; OA articles are governed by the applicable Creative Commons License

cyclic loading. The existing database from Hillebrand et al.[2] was used as a basis and was extended with the tests from Section 3. The evaluated design approaches are EC2 without and with the national annex of Germany,[16,17] the TA of lattice girders in Germany[9,11] and the draft of the prEC2.[18] Since the resistance of the shear reinforcement was the focus of the tests, concrete failure was not considered.

The own investigations with mechanically roughened surfaces (Figure 3) were treated like rough interfaces in the database evaluation, although the actual roughness was smaller than the required value $R_t = 1.5$ mm.[7] One important result of the test series is, that an opening or displacement of these roughened interfaces did not occur under cyclic fatigue loading.

The database contains 72 test specimens. An overview of the test specimens taken from the literature is given in Wieneke.[19] The calculated stress ranges are determined from the applied loads in the tests using the equations of the design approaches in Section 2. In order to evaluate the different design approaches, the calculated stress ranges $\Delta\sigma_{calc}$ of the design approaches for the applied shear force ranges ΔV during the tests are related to the permitted stress ranges $\Delta\sigma_{Rsk}$ according to the S–N curve of TA for the applied load cycles N_{test}. For this purpose, the characteristic value of the permissible stress range $\Delta\sigma_{Rsk}$ was determined with the S–N curve of TA using the number of load cycles N_{test} achieved in the test. For each test the ratio of $\Delta\sigma_{calc}/\Delta\sigma_{Rsk}$ is plotted on the vertical axis over the load cycles of each test on the horizontal axis. A ratio $\Delta\sigma_{calc}/\Delta\sigma_{Rsk}$ larger than 1.0 means, that the calculated stress range $\Delta\sigma_{calc}$ of the design approach is larger than the stress range of the test specimen. For a ratio of 1.0, the result of the design approach would match with the test. For a better comparison of the different approaches, trend lines are given. It should be noted that the database evaluation contains numerous run-throughs. The tests were stopped after a certain number of load cycles, since no indication of cyclic failure could be detected. For these tests, it can therefore be assumed that the characteristic value of the permissible stress range $\Delta\sigma_{Rsk}$ would decrease, if the test had been continued and a higher number of load cycles were reached, which means that the ratios of $\Delta\sigma_{calc}/\Delta\sigma_{Rsk}$ would be larger.

4.2 | Interface shear

The verification of the interface shear under cyclic loads differs between the approaches presented in Section 2.2. While EC2 proposes to calculate with 50% of the adhesion (Equation 3), in TA, EC2 + NA(D), and prEC2, adhesion is completely neglected in the design (Equations 2, 4, and 5). On the other hand, the latter approaches implement additional factors for the resistance of the reinforcement, which reduce its stresses. Figure 24a compares EC2 and EC2 + NA(D). EC2 + NA(D) neglecting the adhesion leads to a higher calculated stress range $\Delta\sigma_{calc}$ EC2 + NA(D). Although the factor 1.2 for the resistance of the reinforcement reduces the stresses of the reinforcement, the increase due to the neglected adhesion has a greater impact and results in a higher calculated stress range $\Delta\sigma_{calc}$.

Compared to EC2, the approach according to TA leads to more economical results (Figure 24b). However, the calculated stresses are still overestimated by more than two times on average. As in EC2 + NA(D), this approach also neglects adhesion. According to TA interfaces are to be designed at least as rough when fatigue loading is present. Therefore, the coefficient of friction for rough interfaces is already included in Equation (2). Furthermore, the calculated stress range is reduced, since the fatigue-effective stress of the shear reinforcement is only 60% of the stress for a 45° truss model according, to TA.[41] The coefficient of friction and the stress range reduction are included in factors 1.4 and 1.67.

According to prEC2 (Equation 5) the cyclic interface shear is represented more accurately than according to TA. The adhesion is assumed to be zero as in the TA and interfaces are to be designed at least as rough when fatigue loading is present. In this approach, the fatigue-effective stress is reduced to 45%. The corresponding related calculated stress ranges of the interface reinforcement are shown in Figure 24c.

4.3 | Shear

The fatigue shear design according to EC2 assumes an increase in the compression strut angle θ (Section 2.3; Equation 6), which is intended to consider a reduced mechanism of the crack friction due to degradation of the crack edges as a result of cyclic loading. The National Annex of Germany, TA and prEC2 adopt this approach of θ_{fat} (Equation 6), so that there is no difference in the verification of the cyclic resistance. However, two different approaches are used for the definition of the monotonic compression strut angle θ, which is the input value for Equation (6). According to EC2 and prEC2 θ can be chosen in the limits of Equation (8), EC + NA(D) and TA give modified limits according to Equation (9).

Figure 25a shows the ratios of the calculated stress ranges according to EC2 + NA(D) and TA in relation to the characteristic permissible stress ranges of the S–N curve according to TA in dependency of the load cycles

17517648, 0, Downloaded from https://onlinelibrary.wiley.com/doi/10.1002/suco.202400219 by Rwth Aachen Hochschulbibliothek, Wiley Online Library on [19/08/2024]. See the Terms and Conditions (https://onlinelibrary.wiley.com/terms-and-conditions) on Wiley Online Library for rules of use; OA articles are governed by the applicable Creative Commons License

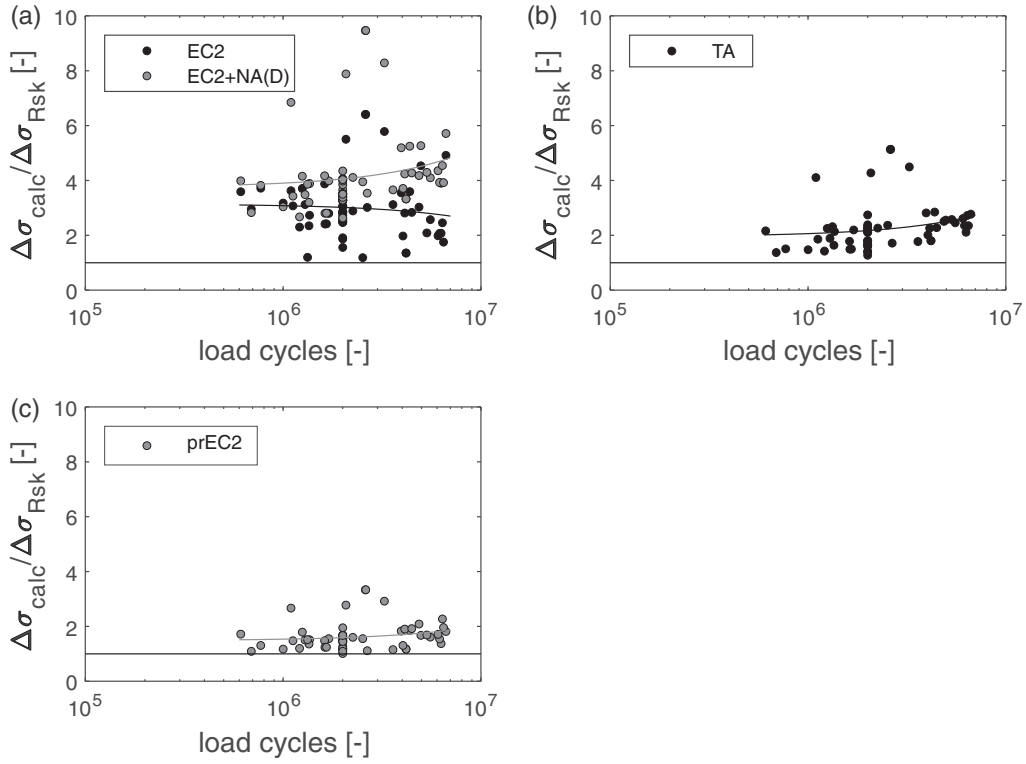


FIGURE 24 Calculated stress ranges of the interface reinforcement $\Delta\sigma_{calc}$ according to (a) Eurocode 2 (EC2) with and without national annex of Germany, (b) the Technical Approval (TA), and (c) new Eurocode 2 (prEC2) related to the permissible stress range $\Delta\sigma_{Rsk}$ according to the *S*–*N* curve of the lattice girders from TA[41] in dependency of the load cycles of the test specimens.

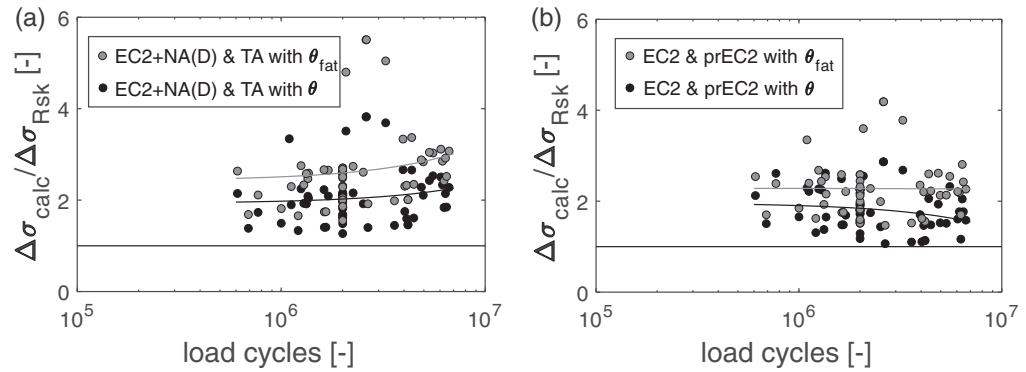


FIGURE 25 Related calculated stress ranges of the shear reinforcement according to (a) Eurocode 2 (EC2) + NA(D) and Technical Approval and (b) EC2 and new Eurocode 2 (prEC2).

of the test specimens. In Figure 25b, the approaches according to EC2 and prEC2 are applied. In addition to the compression strut angle θ_{fat}, the evaluations were also carried out with the monotonic compression strut angle θ, following the proposal of investigations for shear reinforcement in prestressed concrete beams in Teworte and Hegger.[21] The approaches with θ_{fat} significantly overestimate the calculated stress range, whereby the approach according to EC2 and prEC2 provide slightly better results compared to EC2 + NA(D) and TA, especially for high numbers of load cycles. In comparison, the approach with the monotonic compression strut angle θ gives even better results. While the approach of the monotonic compression strut angle overestimates the stress range by a factor of 2.0 on average, the compression strut angle for the cyclic design overestimates it by a factor of 2.7 for EC2 + NA(D) and TA. For EC2 and prEC2, the calculated stress ranges are on average 1.8 times higher than the permissible stress range for the monotonic compression strut angle. For the cyclic compression strut angle approach, this value is approximately 2.3.

17517648, 0, Downloaded from https://onlinelibrary.wiley.com/doi/10.1002/suco.202400219 by Rwth Aachen Hochschulbibliothek, Wiley Online Library on [19/08/2024]. See the Terms and Conditions (https://onlinelibrary.wiley.com/terms-and-conditions) on Wiley Online Library for rules of use; OA articles are governed by the applicable Creative Commons License

5 | SUMMARY

In semi-precast constructions, lattice girders act as interface, shear, and/or punching shear reinforcement when installed as connection between prefabricated elements and *in situ* concrete. Although most semi-precast slabs with lattice girders are loaded monotonically, cyclic loading can be decisive for industrial structures and bridges. Then, conservative design approaches against shear and interface shear fatigue lead to uneconomical results.

To investigate the fatigue behavior for shear and interface shear of semi-precast slabs with lattice girders under cyclic fatigue loading, theoretical and experimental investigations were carried out. Shear slenderness, shear reinforcement ratio, concrete strength, slab depth, as well as the detailing of the support were the main parameters of the study.

The results of 16 specimens tested under cyclic loading can be summarized as follows:

- Despite high upper shear forces V_{max} and large shear force ranges ΔV under cyclic fatigue loading, in test specimens with rough interfaces, no fatigue failure of the shear or interface shear reinforcement could be detected. In slabs with very smooth interfaces, individual fatigue failures of the lattice girders were observed, which did not lead to slab failure. Only in tests with very smooth interfaces a separation between the prefabricated slab and the *in situ* concrete could be detected. If a slab failure under cyclic loading occurred, it was caused by an anchorage failure of the lattice girders.
- For cyclic tests with no indication of fatigue failure after a high number of load cycles, the residual shear resistance was determined. There was no reduction in the monotonic shear resistance caused by the applied cyclic loading.
- The measured stress ranges in the diagonal and vertical bars of the lattice girders were significantly smaller than expected, according to the design approaches. During the cyclic tests, large permanent deflections, crack widths, and steel stresses were observed at unloading to V_{min}, which led to smaller stress ranges in the lattice girder diagonals than calculated. By taking into account the residual stresses in the lattice girders at the lower load V_{min}, the stress range measured in the tests may be represented much better, which will result in a more economical design.
- The tests on single-span slabs with cantilever showed an uncracked concrete zone between the support and the load introduction, where a part of the force is transferred directly into the support. This resulted in even lower stress ranges in the lattice girders. In addition, higher shear capacities could be achieved at the inner support than at the end support when testing the residual shear capacity.
- Despite fatigue fractures in the lattice girder bars, even the slabs with a smooth interface were still able to endure several hundred thousand load cycles. Failure did not occur until the residual static shear resistance was determined. The chosen support detailing, which is frequently used on construction site, generates an additional load-bearing contribution that is not yet considered in the design.
- The database evaluation shows that the shear fatigue verifications for the interface according to EC2 and EC2 + NA(D) are very conservative. The approaches according to TA and prEC2 achieve significantly more accurate results. For the verification of shear fatigue, all approaches give comparable results. The use of a compression strut angle θ instead of θ_{fat} represents the test results better.

These findings illustrate further potential for optimization in the design for shear and interface shear of semi-precast slabs with lattice girders under cyclic fatigue loading. Further investigations are required to quantify all favorable effects in order to improve economic efficiency.

ACKNOWLEDGMENTS

The investigations described in this paper were conducted during a research program initiated by the Research Association of the German Concrete and Precast Industry e. V. and funded by the German Federation of Industrial Research Association (AiF, IGF number 20580N) and the Federal Ministry for Economic Affairs and Climate Action based on a resolution of the German Bundestag. The authors express their thanks to the members of the project committee for the fruitful discussions. Open Access funding enabled and organized by Projekt DEAL.

DATA AVAILABILITY STATEMENT

The data that support the findings of this study are available from the corresponding author upon reasonable request.

ORCID

Matthias Hillebrand https://orcid.org/0000-0001-8215-9987

REFERENCES

1. Furche J, Bauermeister U. Elementbauweise mit Gitterträgern. In: Bergmeister K, Fingerloos F, Wörner J-D, editors. Beton-Kalender 2021: Schwerpunkte: Fertigteile; Integrale Bauwerke. 1st ed. Berlin: Ernst & Sohn; 2021.
2. Hillebrand M, Schmidt M, Wieneke K, Classen M, Hegger J. Investigations on interface shear fatigue of semi-precast slabs

17517648, 0, Downloaded from https://onlinelibrary.wiley.com/doi/10.1002/suco.202400219 by Rwth Aachen Hochschulbibliothek, Wiley Online Library on [19/08/2024]. See the Terms and Conditions (https://onlinelibrary.wiley.com/terms-and-conditions) on Wiley Online Library for rules of use; OA articles are governed by the applicable Creative Commons License

with lattice girders. Appl Sci. 2021;11:11196. https://doi.org/10.3390/app112311196
3. Furche J, Bauermeister U, Kummerow A, Hillebrand M. Durchstanzen bei Ermüdungsbeanspruchung. BuSt. 2019;114:557–64. https://doi.org/10.1002/best.201900012
4. Adam V. Shear in reinforced concrete structures without shear reinforcement – analysis and design. Dissertation. Aachen: RWTH Aachen University. 2021.
5. Adam V, Classen M, Hillebrand M, Hegger J. Shear in continuous slab segments without shear reinforcement under distributed loads. In: Derkowski W, Gwozdziewicz P, Hojdys L, Krajewski P, Pantak M, editors. Fib symposium 2019; 27–29 May, Krakow, Poland. Lausanne: International Federation for Structural Concrete (*fib*); 2019. p. 1771–8.
6. Hegger J, Sherif A, Görtz S. Investigation of pre- and postcracking shear behavior of prestressed concrete beams using innovative measuring techniques. ACI Struct J. 2004;101:183–92.
7. Hillebrand M, Hegger J. Shear and interface shear of semi-precast slabs with lattice girders under monotonic loading. Struct Concr. 2023;24:3055–76. https://doi.org/10.1002/suco.202200423
8. Filigran Trägersysteme GmbH & Co. KG. European Technical Assessment ETA-13/0521: Filigran FDB: Filigran lattice girders as punching reinforcement. Berlin: DIBt.
9. Filigran Trägersysteme GmbH & Co. KG. Allgemeine bauaufsichtliche Zulassung Z-15.1-93: Filigran-EQ-Gitterträger für Fertigplatten mit statisch mitwirkender Ortbetonschicht. Berlin: DIBt.
10. Filigran Trägersysteme GmbH & Co. KG. Allgemeine bauaufsichtliche Zulassung Z-15.2-40: Filigran-D- und/oder Filigran-E- und/oder Filigran-EW- und/oder Filigran-SE/SE2- und/oder Filigran-SWE- und Filigran-EQ-Gitterträger und Anwendungsbestimmungen für wandartige Bauwerksstrukturen aus Elementwänden bei Verwendung dieser Bewehrung. Berlin: DIBt.
11. Badische Drahtwerke GmbH. Allgemeine bauaufsichtliche Zulassung Z-15.1-38: Kaiser-Omnia-Träger KTS für Fertigplatten mit statisch mitwirkender Ortbetonschicht. Berlin: DIBt.
12. Baustahlgewebe GmbH. Allgemeine bauaufsichtliche Zulassung Z-15.2-100: Gittertraeger KT 800, KT900 oder KTE und Anwendungsbestimmungen für wandartige Bauwerksstrukturen bei Verwendung dieser Bewehrung. Berlin: DIBt.
13. Baustahlgewebe GmbH. Allgemeine bauaufsichtliche Zulassung Z-15.2-9 Gitterträger KTW 200 oder KTW 300 und Anwendungsbestimmungen für wandartige Bauwerksstrukturen bei Verwendung dieser Bewehrung. Berlin: DIBt.
14. Baustahlgewebe GmbH. Allgemeine bauaufsichtliche Zulassung Z-15.1-136 Gitterträger KT 100 für Fertigplatten mit statisch mitwirkender Ortbetonschicht (Montaquick-Fertigplatten). Berlin: DIBt.
15. Intersig NV. Allgemeine bauaufsichtliche Zulassung Z-15.1-143: Intersig-EQ-Gitterträger. Berlin: DIBt.
16. Deutsches Institut für Normung e.V. (DIN). Eurocode 2: design of concrete structures – part 1-1: General rules and rules for buildings: German version EN 1992-1-1:2004 + AC.
17. Deutsches Institut für Normung e.V. (DIN). National annex – nationally determined parameters – Eurocode 2: Design of concrete structures – part 1-1: general rules and rules for buildings.
18. CEN/TC 250/SC 2/WG 1. prEN 1992-1-1/2021-09: Eurocode 2: design of concrete structures - part 1–1: general rules for buildings, bridges and civil engineering structures 2021. Stable version by Project Team SC2.T1.
19. Wieneke KM. Horizontal shear design of concrete interfaces in beam and slab structures. Dissertation. Aachen: RWTH Aachen University. 2019.
20. Frey RP, Thürlimann B. Ermüdungsversuche an Stahlbetonbalken mit und ohne Schubbewehrung. Basel: Birkhäuser Basel; 1983.
21. Teworte F, Hegger J. Ermüdung von Spannbetonträgern mit Bügelbewehrung unter Querkraftbeanspruchung. BuSt. 2013;108:475–86. https://doi.org/10.1002/best.201300032
22. Hillebrand M, Hegger J. Fatigue testing of shear reinforcement in prestressed concrete T-beams of bridges. Appl Sci. 2020;10:5560. https://doi.org/10.3390/app10165560
23. Hillebrand M, Teworte F, Hegger J. Shear fatigue of prestressed I-beams with shear reinforcement. Struct Concr. 2021;22:1085–99. https://doi.org/10.1002/suco.202000187
24. Kani GNJ. The riddle of shear failure and its solution. J Am Concr Inst. 1964;61:441–67. https://doi.org/10.14359/7791
25. Islam MS, Pam HJ, Kwan AKH. Shear capacity of high strength concrete beams with their point of inflection within the shear span. Proc Inst Civil Eng – Struct Build. 1998;128:91–9.
26. Tue NV, Tung ND. Study on the influence of M/V-combination on the shear behaviour of slender reinforced concrete beams without stirrups. In: Bayrak O, Fernández Ruiz M, Kaufmann W, Muttoni A, editors. Towards a rational understanding of shear in beams and slabs: fib bulletin 85: workshop in Zürich, Switzerland, September 2016. Lausanne: Fédération Internationale du Béton (*fib*); 2018. p. 100–20.
27. Classen M. Shear crack propagation theory (SCPT) – the mechanical solution to the riddle of shear in RC members without shear reinforcement. Eng Struct. 2020;210:110207. https://doi.org/10.1016/j.engstruct.2020.110207
28. Herbrand M, Hegger J. Experimentelle Untersuchungen zum Einfluss einer externen Vorspannung auf die Querkrafttragfähigkeit vorgespannter Durchlaufträger. Bauingenieur. 2013;88:428–37.
29. Teworte F, Herbrand M, Hegger J. Structural assessment of concrete bridges in Germany—shear resistance under static and fatigue loading. Struct Eng Int. 2015;25:266–74. https://doi.org/10.2749/101686615X14210663188411
30. Gleich P, Maurer R. An analytical model to determine the shear capacity of prestressed continuous concrete beams. IABSE congress, Stockholm 2016: challenges in design and construction of an innovative and sustainable built environment; 21–23 September 2016, Stockholm, Sweden. Zurich: International Association for Bridge and Structural Engineering (IABSE); 2016. p. 1544–55. https://doi.org/10.2749/stockholm.2016.1539
31. Wieneke K, Classen M, Hegger J. Elementdecken mit Gitterträgern unter zyklischer Belastung. BuSt. 2017;112:579–88. https://doi.org/10.1002/best.201700039
32. Hegger J, Wieneke K. Ermüdung von Elementdecken mit Gitterträgern: Abschlussbericht zum IGF-Forschungsvorhaben 18407 N/1. Aachen: Institute of Structural Concrete, RWTH Aachen University; 2017.
33. Wieneke K, van Elten L, Claßen M, Hegger J. Ermüdung von Elementdecken mit Gitterträgern: Wöhlerlinien für Gitterträger. BuSt. 2017;112:723–33. https://doi.org/10.1002/best.201700047
34. Kaufmann N. Das Sandflächenverfahren. Strassenbau-Technik; Köln (Cologne): Müller; 1971. p. 131–5.
35. Wieneke K, Herbrand M, Vogler N, Schwermann R, Blankenbach J. Messverfahren zur Bestimmung der Rautiefe von Betonoberflächen. Bauingenieur. 2018;93:365–73. https://doi.org/10.37544/0005-6650-2018-09-65
36. Hegger J, Hillebrand M. Ermüdung von Elementdecken mit Gitterträgern an Einfeld- und Durchlaufträgern: Abschlussbericht zum IGF-Forschungsvorhaben 20580 N/1. Aachen. 2022.

17517648, 0, Downloaded from https://onlinelibrary.wiley.com/doi/10.1002/suco.202400219 by Rwth Aachen Hochschulbibliothek, Wiley Online Library on [19/08/2024]. See the Terms and Conditions (https://onlinelibrary.wiley.com/terms-and-conditions) on Wiley Online Library for rules of use; OA articles are governed by the applicable Creative Commons License

37. Hohberg R. Zum Ermüdungsverhalten von Beton. Dissertation. Berlin: TU Berlin; März. 2004.
38. Isojeh B, El-Zeghayar M, Vecchio FJ. Simplified constitutive model for fatigue behavior of concrete in compression. J Mater Civ Eng. 2017;29:04017028. https://doi.org/10.1061/(ASCE)MT.1943-5533.0001863
39. Baktheer A, Chudoba R. Experimental and theoretical evidence for the load sequence effect in the compressive fatigue behavior of concrete. Mater Struct. 2021;54. https://doi.org/10.1617/s11527-021-01667-0
40. Wieneke K, Hegger J. Fatigue of semi-precast slabs with lattice girders. In: Hordijk DA, Luković M, editors. Fib symposium 2017; 12–14 June, v. Cham: Springer International Publishing; 2017. p. 921–8. https://doi.org/10.1007/978-3-319-59471-2_107
41. Furche J, Bauermeister U. Elementdecken bei nicht vorwiegend ruhender Belastung. Hinweise zur Anwendung von Gitterträgern nach Zulassung. Beton- Und Stahlbetonbau. 2006; 101:652–62. https://doi.org/10.1002/best.200600494

AUTHOR BIOGRAPHIES



Matthias Hillebrand, Institute of Structural Concrete, RWTH Aachen University, Mies-van-der-Rohe-Strasse 1, 52074 Aachen, Germany. Email: mhillebrand@imb.rwth-aachen.de.



Annkathrin Sinning, Institute of Structural Concrete, RWTH Aachen University, Mies-van-der-Rohe-Strasse 1, 52074 Aachen, Germany. Email: asinning@imb.rwth-aachen.de.



Josef Hegger, Institute of Structural Concrete, RWTH Aachen University, Mies-van-der-Rohe-Strasse 1, 52074 Aachen, Germany. Email: jhegger@imb.rwth-aachen.de.

How to cite this article: Hillebrand M, Sinning A, Hegger J. Shear and interface shear fatigue of semi-precast slabs with lattice girders under cyclic loading. Structural Concrete. 2024. https://doi.org/10.1002/suco.202400219

17517648, 0, Downloaded from https://onlinelibrary.wiley.com/doi/10.1002/suco.202400219 by Rwth Aachen Hochschulbibliothek, Wiley Online Library on [19/08/2024]. See the Terms and Conditions (https://onlinelibrary.wiley.com/terms-and-conditions) on Wiley Online Library for rules of use; OA articles are governed by the applicable Creative Commons License